



Regular Articles

Efficient fragmentation-aware algorithms for multicast traffic in elastic optical networks with a novel demand size based fragmentation metric

Leila Asadzadeh^a, Ahmad Khonsari^{a,b,*}, Akbar Ghaffarpour Rahbar^c^a School of Electrical and Computer Engineering, University of Tehran, Tehran 14155-6619, Iran^b School of Computer Science, Institute for Research in Fundamental Sciences, Institute for Research in Fundamental Sciences, Tehran 19538-33511, Iran^c Computer Networks Research Lab, Faculty of Electrical Engineering, Tabriz University of Technology, Tabriz, Iran

ARTICLE INFO

Keywords:

Elastic optical networks
Multicast transmission
Multicast routing
Modulation level and spectrum assignment
Fragmentation metrics

ABSTRACT

With flexible allocation of spectrum resources and on-demand bandwidth provisioning, Elastic Optical Networks (EONs) have made it possible to meet the high volumes of traffic demands. Multicast Routing, Modulation level and Spectrum Assignment (MRMSA) algorithms are important in efficient multicast transmissions in EONs. The dynamic nature of allocating and releasing spectral resources causes the spectrum to be divided into small empty blocks that are not suitable to be allocated anymore, so the resource utilization reduces greatly. Many metrics have been introduced in the literature to measure the amount of fragmented spectrum. In this paper, we propose a novel demand size based fragmentation metric (DemFRAG) to evaluate the suitability of the optical links or paths to establish the requests. We also propose two fragmentation-aware algorithms based on this novel metric to efficiently solve MRMSA problem in EONs. The performance of the proposed fragmentation-aware MRMSA algorithms is evaluated by considering the novel DemFRAG metric and also other fragmentation metrics in terms of Blocking Probability (BP) and Bandwidth Blocking Probability (BBP) under different network topologies. Simulation results demonstrate that the proposed MRMSA algorithms with the DemFRAG metric allow for significant reduction in BP and BBP compared to other algorithms.

1. Introduction

With the ever-increasing growth of traffic requests, the need for high bandwidth networks has increased a lot. Services like IP Television (IPTV), Content Delivery Network (CDN) data distribution, transmission of scientific data, and big data transmission have high bandwidth requirements of up to 10–200 Gbps [1]. Elastic Optical Network (EON) with efficient and flexible allocation of spectrum resources in optical fiber links and on-demand bandwidth provisioning makes it possible to respond to this high volumes of traffic demands. Unlike Wavelength Division Multiplexing (WDM) networks, in EON, each demand is allocated exactly the requested amount of spectrum resources, and in this way, the waste of resources is minimized. Bandwidth Variable Transponders (BVTs) equipped at EON nodes can operate at a set of possible bit-rates and employ a set of modulation formats at any bit-rate. Therefore, the number of adjacent Frequency Slots (FSs) required for a request using a given modulation format can be computed [2]. Thus, EONs allow flexible and dynamic selection of the modulation formats. This feature allows more efficient usage of the spectrum by allocation of more spectrally efficient modulation formats when the quality of signal

does not undergo any serious physical impairment along its path. This feature, called Distance Adaptive Transmission (DAT), is one of the key differences between EON and WDM [3].

An Sliceable Bandwidth Variable Transponder (SBVT) has the capability to allocate its capacity into one or several optical flows that are transmitted to one or several destinations. Therefore, when an SBVT is used to generate a low bit rate channel, its idle capacity can be exploited for transmitting other independent data flows. An SBVT generates multiple optical flows that can be flexibly associated with the traffic coming from the upper layers according to traffic requirements. Therefore, optical flows can be aggregated or can be sliced based on the traffic needs [4].

The resource allocation in EON consists of determining the links, spectrum range and modulation format of the signal at the transmitter. In spectrum allocation, three constraints should be considered: spectrum contiguity constraint, spectrum continuity constraint and non-overlapping spectrum assignment. If a demand requires t units of spectrum, then t contiguous subcarrier slots must be allocated to it (due to the spectrum contiguity constraint), and the same t contiguous slots

* Corresponding author at: School of Computer Science, Institute for Research in Fundamental Sciences, Institute for Research in Fundamental Sciences, Tehran 19538-33511, Iran.

E-mail addresses: lasadzadeh@ut.ac.ir (L. Asadzadeh), a_khonsari@ut.ac.ir (A. Khonsari), ghaffarpour@ut.ac.ir (A. Ghaffarpour Rahbar).

<https://doi.org/10.1016/j.yofte.2025.104233>

Received 22 December 2024; Received in revised form 9 March 2025; Accepted 6 April 2025

Available online 22 May 2025

1068-5200/© 2025 Published by Elsevier Inc.

must be allocated on each link along the route of the demand (due to the spectrum continuity constraint) [4]. Non-overlapping spectrum assignment implies that one frequency slot can be employed by only a single connection request at a time and the allocated frequency slots to different connection requests must be separated by guard-bands.

Some applications such as video streaming, database synchronization among distributed datacenters and cloud computing need to send traffic from one source to multiple destinations in the network, which is known as multicasting. Multicasting is a form of communication that simultaneously transmit data traffic from a source to a set of destinations in an efficient manner, so that creating a multicast tree is much more efficient than creating a couple of unicast lightpath [5]. Multicast Routing and Spectrum Assignment (MRSA) and Multicast Routing, Modulation level and Spectrum Assignment (MRMSA) are two important problems in EONs, thus many research efforts have been done to effectively solve these problems.

The fulfillment of the continuity and contiguity constraints, together with the allocation and de-allocation of FSs to connection requests, may cause fragmentation, i.e., the appearance of isolated idle FSs, almost unusable for the establishment of new connections, thereby increasing blocking events [6]. Various approaches have been proposed to deal with this problem in recent years and many metrics for measuring the amount of fragmented spectrum have been proposed such as External Fragmentation (EF) [7], Normalized Path Fragmentation Rate [8] (NPPR), Golden metric [9] and Fragmentation Measure Metric (FMM) [10].

Our objective in this article is to reduce Blocking Probability (BP) and Bandwidth Blocking Probability (BBP) by proposing the Least Fragmented Path based Tree MRMSA (LFPT-MRMSA) and Optimal Least Fragmented Tree MRMSA (OLFT-MRMSA) algorithms in order to routing, modulation level and spectrum assignment for dynamic multicast traffics with high data rates (300–900 Gbps). We focus on the MRMSA problem in EONs with multicast-capable switches and propose new heuristic approaches to efficiently solve the problem. We also introduce a new fragmentation metric called demand size based fragmentation metric (DemFRAG) that evaluates the fragmented spectrum on the links or paths by considering the amount of required traffic of the incoming multicast request.

In the Least Fragmented Path based Tree MRMSA (LFPT-MRMSA) algorithm, the list of shortest paths from the source node to each one of the destination nodes is sorted according to the fragmentation values calculated by using the DemFRAG metric, and then the multicast tree is constructed based on the sorted lists. In the Optimal Least Fragmented Tree MRMSA (OLFT-MRMSA) algorithm, the optimal multicast tree that has the least amount of fragmentation among all the constructed trees is selected and the multicast request is established on it. The performance of the proposed fragmentation-aware algorithms is evaluated by considering the novel DemFRAG metric and also other fragmentation metrics introduced in the literature and the BP and BBP values are compared for different requested traffics at various network loads under the NSFNET and JPN12 topologies.

The remainder of this paper is organized as follows. In Section 2, we discuss related works and describe some of the fragmentation metrics introduced in the literature. Multicast routing, modulation level and spectrum assignment problem is explained in Section 3. Our fragmentation-aware MRMSA algorithms and the proposed novel demand size based fragmentation metric (DemFRAG) are presented in Section 4. We describe simulation results of the proposed MRMSA algorithms in Section 5. Conclusion will be expressed in Section 6.

2. Related work

As one of the crucial problems for EON, the Multicast Routing, Modulation level and Spectrum Assignment (MRMSA) has been widely investigated. MRMSA can be considered as three sub-problems: multicast routing, modulation level selection and spectrum assignment.

Different methods for implementation of multicast routing in EONs which have been widely used are light-tree, light-forest, light-trail and lightpath. We can summarize these methods as follows.

- **Light-tree.** A light-tree is created from the source node to all the destination nodes using the Minimum Spanning Tree (MST) or Shortest Path Tree (SPT) algorithms. Therefore, the light-tree is considered a point-to-multipoint channel. The same frequency slots on all links of the created light-tree must be assigned to the multicast request. The light-tree structure can be used when the network nodes are equipped with multicast-capable switches [11], [12,13].
- **Light-forest.** A multicast request is fulfilled by several light-trees so that each light-tree covers only a part of the destination set [14–16].
- **Light-trail.** A light-trail is based on the Tap-and-Continue (TaC) concept where the nodes between the two end nodes of the trail can also receive the signal by tapping a small portion of the power, while switching the remainder to the output. To perform optical multicasting, a path must be determined that starts from the source node and passes through all the destination nodes [17, 18].
- **Lightpath.** Since multicast-capable switches usually have complex structures and can be very expensive, it will be interesting to investigate overlay multicasting in which a logical light-tree is constructed for the multicast request and multiple unicast lightpaths are created to actually implement it. Therefore, cost-effective network planning and provisioning will be possible especially when multicast traffic is not dominant [1,19–21].

A new algorithm based on EON was proposed that employs a sub-tree based scheme to establish multicast transmissions [3]. The authors take into account the effects of splitting a transient light at intermediary nodes based on the signal-to-noise ratio to enhance the accuracy of the resource allocation. In [11], authors proposed algorithms for generation of candidate trees for EON multicasting and quality of the obtained sets of candidate trees was evaluated by running a Routing and Spectrum Assignment (RSA) algorithm.

Authors in [5] proposed an efficient scheme, namely Optical Load-balanced Multicast Routing with Admission Control (OLMR-AC), to improve the wavelength resources utilization in the network. As an advantage, OLMR-AC jointly considers both distance and congestion factors to create a multicast session. For each admitted session, a bandwidth-guaranteed steiner tree is provided in which not only the source node has a minimum-cost path to each receiver, but also its overall cost is minimal. The effectiveness, in term of spectrum and transmitter usage, among light-trail, light-path and the light-tree in multicast accommodation were compared and the benefit of having distance-adaptive transmission for these approaches was evaluated in [17]. Cai et al. [18] consider using the light-trail technology for the accommodation of multicast requests in elastic optical networks with adaptive modulation. For better spectrum efficiency, they consider accommodating each multicast by multiple light-trails.

A novel Distributed Sub-Tree based Optical Multicasting (DST-OM) scheme was proposed in [15] and an integer linear program model was developed for the DST-OM scheme with the aim of minimizing the total spectrum consumption of all multicast demands in elastic optical data center networks. Fan et al. [16] propose and investigate a sub-tree scheme for All-Optical Multicast Routing, Modulation level and Spectrum Allocation (AOM-RMSA) in EONs. A multicast request is accommodated by several light-trees and each light-tree covers only a part of the destination set. They propose two time-efficient heuristic algorithms that construct sub-trees according to the link-sharing ratio between the paths from source to two distinct destinations. The proposed algorithms improve the spectrum utilization by building sub-trees that have smaller tree-spanning size and adopt higher-level modulation formats.

In [12], dynamic resource allocation and multicast routing algorithms are proposed for EONs. The proposed algorithms find the shortest path trees by modeling either the amount of free spectrum in each link or the link length as the cost function of routing method. Simulation results reveal that considering the cost function of routing algorithm based on the available spectrum in each link will improve the blocking probability while reduce the spectrum efficiency. On the other hand, by considering link length as the cost function, the blocking probability becomes worsen whereas the bandwidth efficiency is improved.

In [13], authors have proposed a light-tree sharing based multicast routing and spectrum assignment technique. Similar multicast requests are grouped together and their bandwidth requirements are added up. For each multicast session request, a layered auxiliary graph is selected based on the available spectrum in the network and the request's bandwidth demand. An efficient light-tree is generated from this auxiliary graph, first for the clubbed request and then for the individual requests separately. The simulation results show that the proposed algorithm significantly reduces the average tree size and increases the number of requests satisfied than the well-known existing algorithm mentioned in literature. Incidentally the average number of splitters required is also reduced.

Application layer overlay networks though built on top of the physical network, behave like an independent virtual network made up of only logical links between the nodes. Several authors have proposed systems, mechanisms and protocols for the implementation of multicast media streaming over overlay networks [19]. Liu et al. [20] studied Overlay Multicast (OL-M) in multicast-incapable EONs, and proposed the Spectrum-Flexible Member-Only Relay (OL-M-SFMOR) scheme. Their simulation results indicated that OL-M-SFMOR achieves significant improvements on the spectrum-efficiency of multicast traffic in EONs, when compared with other multicast schemes, even including the all-optical multicast schemes in multicast-capable EONs.

In [21], authors assume that the overlay network is deployed to provide multicasting Deadline-Driven Requests (DDRs), which require to transmit given amount of data before data-transfer deadline is up. They considered a multilayer optimization problem that combines two approaches — optimization of an overlay dynamic multicasting sessions and next provisioning of created overlay multicasting trees as a sets of unicast demands in the underlying optical layer. The authors in [1] have addressed overlay multicasting problem with the survivability assumptions and have proposed several survivability scenarios that can be applied in the network to provide the required protection against failures.

In [22], authors incorporate a layered approach to design integrated Multicast-Capable Routing and Spectrum Assignment (MC-RSA) algorithms for achieving efficient all optical multicasting in spectrum-sliced EONs. The simulation results demonstrate that compared to the existing MC-RSA algorithms, their approaches achieve more efficient network planning in terms of spectrum utilization, and provide lower blocking probabilities in network provisioning.

In [23], the authors have proposed a novel Multicast Two-part Two-path Two-direction Allocation (MT^3A) scheme in order to routing, spectrum and modulation-level assignment for dynamic multicast traffic in EONs. With this scheme, each sub-request related to a multicast request is divided into two parts considering the property of Sliceable Bandwidth Variable Transponders (SBVTs) and is set up in two different directions in two different lightpaths. By using the MT^3A scheme compared to comparative schemes, with increasing the data rate, BBP is reduced. In [24], authors investigate efficient allocation of three types of flows (unicast, anycast, multicast) in EON with dedicated path protection.

Walkowiak et al. [25] propose three new approaches for optimization of multicast traffic in EONs that implement distance-adaptive transmission. Two of the approaches are based on integer linear programming modeling, whereas the last one is an effective heuristic. The

algorithms based on candidate tree modeling of multicasting outperform other methods for larger problem instances in terms of spectrum usage and applicability. In [26], authors investigate multicasting over spectrum elastic optical networks by developing two heuristic algorithms. The multicast performance over elastic optical networks is compared to that over ITU-T grid-based WDM optical networks.

In [27], authors present an approximation based Steiner Tree Approach for RSA (STA-RSA) and compare it with the Shortest Path Tree based Routing and Spectrum Allocation (SPT-RSA) to show the benefits of STA-RSA over SPT-RSA. The numerical results show that the presented approach outperforms the traditional approaches in terms of bandwidth blocking probability.

In order to further optimize the EON, [28] uses the least connections algorithm to solve the EON load balancing problem, taking into account the different server load capacity to improve it. In addition, to further improve the performance of EON, this paper combines Genetic Algorithm, improved Least Connections algorithm and Ant Colony algorithm to propose a new algorithm LC-GAACO. The simulation results show that the LC-GAACO algorithm will consume more optical transceivers while taking into account load balancing, but the network load balancing effect, network spectrum utilization, and blocking rate are better than traditional algorithms.

Qiu [29] proposed a Time-based Composite-Consumption Aware (TCCA) MRSA algorithm to optimize both the fragmented and the allocated resources consumed by the multicast transmission in EONs. By additionally taking the holding time of each multicast service request into account, the proposed algorithm can comprehensively optimize both the fragmented and the allocated resource consumption for the multicast transmission in EONs.

In [30], authors focus on the problem of routing, modulation level selection, spectrum, and transceiver assignment for multicast services with different security levels. They study potential performance gains resulting from applying a distributed sub-tree scheme to multi-class multicast service aggregation, realizing reduced overall cost.

Aibin et al. [31] compare various protection methods that may be applied to protect multicast sessions in EONs. For this purpose, they adapt two dynamic routing algorithms with additional survivability constraints and the possibility to change the modulation format at the regeneration nodes. They compared three approaches for survivable multicasting in EONs, these are: dedicated path protection, shared backup path protection and segment-based protection.

Since a multicast service can be hosted in multiple geographically-distributed data-centers in an Elastic Optical Data-Center Network (EO-DCN), Gao et al. [32] construct several Distributed Sub-Light-Trees (DSLTTs) to serve the users of a multicast request. Further, they protect each source-destination pair of a primary DSLTT by a link-disjoint backup path against any link failure. Spectrum resource can be shared among the backup paths of different multicast requests or among the primary paths and the backup paths of the same multicast request if they do not fail simultaneously.

Cai et al. [33] consider the Routing and Spectrum Allocation (RSA) problem of protecting all-optical multicast sessions against a single link failure in elastic optical networks. They use a scheme to protect each of the paths by an arc-disjoint backup path in the case of any link failure. For this problem, they provide a node-arc Integer Linear Programming (ILP) formulation and propose a heuristic algorithm for this protection scheme and evaluate the improvement achieved by the flexible grids adopted in EONs over the fixed-grid WDM networks. Based on the studied scenarios, consistent improvement in efficiency of flexible grid EONs over fixed-grid WDM networks has been observed.

In order to guarantee the reliability and increase the efficiency of the multicast transmission in EONs, Pan et al. [34] proposed a Multiple Leaf-Ringing based Protection algorithm with Spectrum Defragmentation (MLRP-SD). The proposed algorithm firstly sorts the destination nodes of a multicast service into multiple groups. Then, it constructs

Table 1
Researches about multicasting in EONs.

Reference	Objective	Description
Kmiecik et al. [1]	MRMSA + traffic protection	Two-layer optimization of survivable overlay multicasting in EON
Tarhani et al. [3]	MRMSA	Efficient sub-tree based scheme for multicasting in EON
Aboomasoudi et al. [5]	MRSA + load balancing	Improving acceptance rate of QoS-guaranteed point-to-multipoint traffic flows in EONs
Walkowiak et al. [11]	MRMSA	Calculation of various candidate trees for multicasting in EON
Moharrami et al. [12]	MRMSA	Spectrum-usage-aware resource allocation and multicast routing in EON
Choudhury et al. [13]	MRSA	Multicasting in flexible-grid optical networks based on light-tree sharing approach
Guo et al. [14]	MRMSA	Link-aware distributed steiner subtree scheme for all-optical multicasting in elastic optical data center networks (EO-DCN)
Zhang et al. [15]	MRMSA	Distributed sub-tree based optical multicasting scheme in EO-DCNs
Fan et al. [16]	MRMSA	Distance-adaptive spectrum resource allocation for all-optical multicasting in EON
Cai et al. [17]	MRMSA	Comparison of different multicast approaches in EON
Cai et al. [18]	MRMSA	Multicasting in EONs with multiple light-trails and adaptive modulation
Firdhous et al. [19]	MRMSA	Review on multicasting over overlay networks
Liu et al. [20]	MRMSA	Spectrum-efficient overlay multicasting in multicast-incapable EON
Kmiecik et al. [21]	MRMSA	Dynamic overlay multicasting for deadline-driven requests provisioning in EONs
Liu et al. [22]	MRSA	Design integrated RSA for multicast in EON with a layered approach
Sarraaf et al. [23]	MRMSA	A two-part two-path two-direction allocation multicasting scheme in EON
Gościęń et al. [24]	RMSA + MRMSA + traffic protection	Optimization of unicast, anycast and multicast flows in survivable EON
Walkowiak et al. [25]	MRMSA	Optimization of multicast traffic in EON with distance-adaptive transmission
Wang et al. [26]	MRSA	Performance analysis of multicast traffic over spectrum EON
Choudhury et al. [27]	MRMSA	Performance of routing and spectrum allocation approaches for multicast traffic in EON
Liu et al. [28]	MRSA + load balancing	Research on load balancing algorithm of multicast services based on EON
Qiu et al. [29]	MRMSA	Time based resource-consumption-aware spectrum assignment for multicast traffic in EON
Tang et al. [30]	MRMSA + service aggregation	Multi-class multicast service aggregation in EO-DCNs
Aibin et al. [31]	MRMSA + traffic protection	Different strategies for dynamic multicast traffic protection in EON
Gao et al. [32]	MRMSA + traffic protection	Multicast provisioning with shared protection in EO-DCNs
Cai et al. [33]	MRSA+ traffic protection	Elastic versus WDM networks with dedicated multicast protection
Pan et al. [34]	MRMSA+traffic protection	Protection algorithm with spectrum defragmentation for multicast traffic in EON

one leaf ring for all the destination nodes in one group and two dedicated trunk paths (including one protection trunk path) from the source to each constructed ring. The proposed MLRP-SD algorithm triggers spectrum defragmentation to re-optimize resource utilization in the network when sufficient available spectrum resources cannot be found along the sought protection trunk paths. The simulation results show that the proposed MLRP-SD algorithm can guarantee the reliability of multicast traffic with low service blocking probability. A summary of researches about multicasting in EONs is presented in Table 1.

Dynamic allocation and release of frequency slots to/from connection requests create a new problem called fragmentation that if it is not dealt with correctly, it will cause a waste of spectrum resources. The proposed method in [35] uses a novel fragmentation coefficient based Routing, Spectrum and Core Allocation (RSCA). The aim of the plan is to make sure that the spectrum is used as effectively as possible. The study in [36] presents a new spectrum allocation approach that incorporates path selection and careful consideration of crosstalk (XT) limitations. Authors propose a novel Fragmentation Coefficient and Dynamic Core-Changing-based Routing, Spectrum, and Core Allocation (FC-DCCRSCA) technique. The algorithm begins by searching for the shortest paths using the Dijkstra algorithm. It then proceeds to evaluate Fragmentation Coefficients (FC) using the Continuous Aligned Slot Ratio (CASR) model. In [37] authors design a spectrum fragmentation evaluation model, and based on this model, propose an improved Lowest Fragmentation Fit Dynamic Bandwidth Allocation (LFF-DBA) algorithm to optimize network resource allocation in the Software-Defined Elastic Optical Network (SD-EON). In [38], two

new algorithms are proposed in SDM-EON to improve the fragmentation problem and improve blocking probability, called Priority Select Frequency (P-S-F) and Priority Select Core (P-S-CO). Authors assume that connection demands have three priorities as high-priority, mid-priority, and low-priority and the requested bandwidth of a connection demand is divided into smaller sizes to be setup in multiple cores. Performance evaluation results proved the reduction in connection blocking probability.

In the next subsection, we explain some of the fragmentation metrics that have been used frequently in the literature.

2.1. Fragmentation metrics

The dynamic allocation and release of spectrum resources cause spectrum fragmentation and reduce resource efficiency. There are different metrics proposed in the literature to quantify the fragmented spectrum on links or paths in the EON. In these metrics, the number of available free frequency slots, or the number/size of free frequency blocks, or the position of free and occupied frequency slots, or a combination of these parameters are measured to evaluate the fragmented spectrum on a link or path. Some of the fragmentation metrics that have been used frequently in the literature are as follows:

- **Shannon's Entropy (τ)** [39]: This metric is based on shannons entropy theory and is formulated by Eq. (1):

$$\tau = \sum_{i \in I} \frac{f_i}{S} \ln\left(\frac{S}{f_i}\right) \quad (1)$$

where S denotes the number of slots and f_i denotes the number of the available contiguous slots in block i . A block is a set of free frequency slots on spectrum. Parameters I and τ denote the set of blocks consisting of contiguous slots in each link or path and estimated value for fragmentation, respectively.

- **External Fragmentation (EF)** [7]: The EF metric is quantified by Eq. (2):

$$EF = 1 - \frac{\text{Size of biggest frequency block}}{\text{Total free frequency slots}} \quad (2)$$

- **Normalized Path Fragmentation Rate (NPFR)** [8]: The NPFR metric measures fragmented value of spectrum on a path and is shown in Eq. (3):

$$NPFR = \frac{\left(\sum_{i=1}^{N_f} \frac{1}{\text{size of } i^{\text{th}} \text{ free block}} \right) \times N_f}{\left\lceil \frac{m}{2} \right\rceil^2} \quad (3)$$

where N_f is the number of free frequency blocks on a path and m shows the number of all frequency slots on the path.

- **Fc** [40]: The Fc metric takes into account the fact that fragmentation is dependent on the bandwidth of connection requests. Hence, the fragmentation can also be a function of the number of slots required by a connection request. This metric is expressed in Eq. (4):

$$Fc = 1 - \frac{c \times \text{Free}(c)}{\text{Total free slots}} \quad (4)$$

where c is the number of slots required for a certain connection and $\text{Free}(c)$ is a function that counts the number of simultaneous requests of size c that can be satisfied. In the Fc metric, the amount of fragmented spectrum is calculated based on the number of empty blocks that can be allocated to an input request, and the inappropriate places are ignored.

- **Golden metric** [9]: This metric is a two dimensional metric and takes into account the minimum and maximum value of the required frequency slots of all requests to quantify the fragmentation degree in the network. The fragmentation value of a link, path, or core is calculated based on two dimensions a and b . Suppose that requested slots of demands are between n_1 and n_2 (so that $n_1 < n_2$). For each free frequency block Gap_i , two parameters a_i and b_i are computed as follows:

$$\begin{aligned} &\text{if } \text{size}(Gap_i) < n_1 : a_i = 0, \quad b_i = \frac{-\text{size}(Gap_i)}{\text{average}[n_1, n_2]} \\ &\text{if } \text{size}(Gap_i) > n_2 : a_i = \frac{\text{size}(Gap_i)}{\text{average}[n_1, n_2]}, \quad b_i = 0 \\ &\text{if } n_1 \leq \text{size}(Gap_i) \leq n_2 : a_i = \frac{\text{size}(Gap_i) - n_1 + 1}{\text{average}[n_1, n_2]}, \\ &\quad b_i = \frac{-(n_2 - \text{size}(Gap_i))}{\text{average}[n_1, n_2]} \end{aligned}$$

where $\text{size}(Gap_i)$ is the number of frequency slots in Gap_i and $\text{average}[n_1, n_2]$ is the average of intervals n_1 and n_2 . Finally, for all gaps, the a and b values and the Golden metric are calculated as follows where N is the total number of gaps in a given path, link or core.

$$a = \sum_{i=0}^N a_i, \quad b = \sum_{i=0}^N b_i, \quad \text{GoldenMetric} = \frac{a}{|b|} \quad (5)$$

- **Fragmentation Measure Metric (FMM)** [10]: The FMM measures fragmentation value according to Eq. (6):

$$FMM = \left(\frac{LFFS}{LBFS} \times Gaps \times \frac{|BgstGap \times SBgstGap - SmstGap \times SSmstGap| + 1}{|SBgstGap - SSmstGap| + 1} \right) / 100 \quad (6)$$

where $LFFS$ and $LBFS$ are the index of last full and last blank frequency slot on the path consequently. $Gaps$ indicates the number of free slots on the path. $BgstGap$, $SBgstGap$, $SmstGap$, and $SSmstGap$ are the number of biggest gap and its size and the number of smallest gap and its size on the path consequently.

When we Compare different fragmentation metrics, as illustrated in Table 2, all metrics except Fc do not consider the exact required Frequency Slots (FSs) of incoming request, and thus they are not based on demand size. The Golden metric considers the minimum and maximum values of the required FSs of all requests. The EF and Fc metrics do not take into account all free frequency blocks to evaluate fragmentation status of paths. Among all fragmentation metrics, only the Golden metric considers the negative impact of inappropriate frequency blocks to evaluate paths.

By considering the accurate size of demands, all free frequency blocks, and the negative impact of inappropriate frequency blocks, we propose a more suitable metric for measuring the amount of fragmentation in the paths.

2.2. Motivation and contribution

Dynamic establishment and disruption of connections in the EONs cause the spectrum to find free FSs called fragmented places that are not suitable to be allocated anymore, so the resource utilization reduces greatly. We can establish connections through appropriate paths by defining accurate fragmentation metrics to evaluate fragmented spectrum on paths more precisely. We try to improve the performance of spectrum allocation in EONs by focusing on the fragmentation problem.

By considering Distance Adaptive Transmission (DAT), the number of required FSs for a request is determined based on the length of the selected path for establishing the request, thus required number of FSs will vary on different paths. We propose a novel metric for measuring the degree of fragmentation on paths according to the exact FS requirements of requests determined based on the DAT technique.

Many metrics have been introduced in the literature to measure the amount of fragmented spectrum. From the fragmentation metrics listed in Table 2, only the Fc is based on the size of incoming request but does not consider inappropriate free frequency blocks to evaluate links or paths in the network. The Golden metric considers the negative impact of inappropriate frequency blocks but is not based on the exact size of the request. It uses the minimum and maximum values of required FSs of all incoming requests to the network.

The contribution of this paper is to propose a novel fragmentation metric that not only is based on the size of the requests and takes into account the required FSs on the assumed path but also considers the frequency blocks that are not appropriate for assigning to the request. By considering the accurate size of requests, all free frequency blocks, and the negative impact of inappropriate free frequency blocks, we can measure the fragmented spectrum on the paths more precisely. In other words, for each path, the free frequency blocks that can be allocated and also those that cannot be allocated to the request are calculated based on the number of FSs needed on that path, based on its length, and then the suitability of the path for the request is examined.

Setting up a light-tree that contains all source and destination nodes is one of the most used ways to establish a multicast request from a source node to a set of destination nodes. By introducing a novel demand size based fragmentation metric, we propose two fragmentation-aware heuristic algorithms to solve the MRMSA problem in EONs. Different methods are used in these algorithms for constructing the multicast light-tree. In the proposed fragmentation-aware algorithms, our main objective is to reduce BP and BBP. The main contributions of this paper can be summarized as follows:

- By considering the accurate size of requests, all free frequency blocks, and the negative impact of inappropriate free frequency blocks, we introduce a novel demand size based fragmentation metric named **DemFRAG** to evaluate the fragmented spectrum more precisely. The DemFRAG metric can be used to calculate the amount of fragmentation on the links, paths or cores. We can employ this metric in the point to point and point to multi-point transmission frameworks.

Table 2
Comparison of different fragmentation metrics.

Fragmentation metric	Is based on demand size?	Considers all free blocks?	Considers negative impact of inappropriate blocks?
τ	No	Yes	No
EF	No	No	No
Fc	Yes	No	No
NPFR	No	Yes	No
Golden Metric	No	Yes	Yes
FMM	No	Yes	No
DemFRAG	Yes	Yes	Yes

- We propose the **Least Fragmented Path based Tree MRMSA (LFPT-MRMSA) algorithm** for dynamic multicast requests in EON. In the LFPT-MRMSA algorithm, the multicast light-tree is constructed by considering the least fragmented shortest path for each source and destination node pair based on the proposed DemFRAG metric.
- We propose the **Optimal Least Fragmented Tree MRMSA (OLFT-MRMSA) algorithm** for dynamic multicast requests in EON. In the OLFT-MRMSA algorithm, among various possible multicast light-trees containing source and destination nodes, the least fragmented light-tree is selected based on the proposed DemFRAG metric.
- We compare the performance of the proposed LFPT-MRMSA and OLFT-MRMSA algorithms by considering the novel DemFRAG metric and also other fragmentation metrics in terms of BP and BBP under NSFNET and JPN12 network topologies.
- We show that our proposed novel DemFRAG metric provides significant reductions in BP and BBP compared to other fragmentation metrics.

3. Multicast routing, modulation level and spectrum assignment

With the multicast-capable switches in EON nodes, a light-tree containing the source and destination nodes can be constructed to establish the multicast request. The constructed light-trees for the multicast request may be different depending on the features considered in the tree construction procedure. An example of the construction of multicast light-tree has been depicted in Fig. 1 for a request from the source node A to the destination nodes $\{D, E, F\}$. Three light-trees T_1 , T_2 and T_3 have been created for this request. The path $\{A \rightarrow B \rightarrow D\}$ from A to D , the path $\{A \rightarrow C \rightarrow E\}$ from A to E , and the path $\{A \rightarrow C \rightarrow F\}$ from A to F are used to construct the light-tree T_1 for this multicast request. The path $\{A \rightarrow C \rightarrow D\}$ from A to D , the path $\{A \rightarrow C \rightarrow E\}$ from A to E , and the path $\{A \rightarrow C \rightarrow F\}$ from A to F are used to construct the light-tree T_2 . The path $\{A \rightarrow B \rightarrow D\}$ from A to D , the path $\{A \rightarrow B \rightarrow D \rightarrow E\}$ from A to E , and the path $\{A \rightarrow C \rightarrow F\}$ from A to F are used to construct the light-tree T_3 .

In the Distance Adaptive Transmission (DAT), the modulation level and required FSs for a request can be specified according to the distance between the source and destination node. The modulation levels are $m = 1, 2, 3, 4$ to signify Binary Phase Shift Keying (BPSK), Quadrature Phase Shift Keying (QPSK), 8-Quadrature Amplitude Modulation (8-QAM), and 16-Quadrature Amplitude Modulation (16-QAM). It is assumed that they can support the data rate of 12.5, 25, 37.5, and 50 Gbps per frequency slice. The relation between the modulation levels and transmission reach is depicted in Table 3.

The number of required frequency slots for the request i denoted by FS_{num} is obtained by using Eq. (7) [41]:

$$FS_{num} = \lceil \frac{b_i}{Y_{slot} \times m} \rceil + N_G \quad (7)$$

In Eq. (7), Y_{slot} is the width of one frequency slot and usually is set to 12.5 Gbps, b_i is the requested bandwidth of request i and N_G is the number of guard band slots.

In a multicast light-tree, the modulation level is calculated based on the diameter of the light-tree, i.e. the length of longest path from the source node to destination nodes.

Table 3
Transmission reach of modulation levels.

Modulation level	Transmission reach (km)	Capacity (Gbps)	m
BPSK	Greater than 2500	12.5	1
QPSK	2500	25	2
8-QAM	1250	37.5	3
16-QAM	625	50	4

4. Fragmentation-aware MRMSA algorithms

Fragmentation-aware multicast routing, modulation level and spectrum assignment algorithms try to improve the performance of resource allocation in the network by focusing on the fragmentation problem. By considering fragmentation, we could reduce BP and BBP. To do this, we propose a novel fragmentation metric that can measure the fragmentation degree of paths more precisely and use it in our fragmentation-aware algorithms. Supposing that all nodes in the network are multicast-capable, we design two multicast light-tree construction methods based on the proposed novel fragmentation metric. These algorithms are named as the Least Fragmented Path based Tree Multicast Routing, Modulation level and Spectrum Assignment (LFPT-MRMSA) and Optimal Least Fragmented Tree Multicast Routing, Modulation level and Spectrum Assignment (OLFT-MRMSA).

In Section 4.1, we propose our novel fragmentation metric and present an example. The network model is explained in Section 4.2. We describe our LFPT-MRMSA and OLFT-MRMSA algorithms and explain their details in Sections 4.3 and 4.4.

4.1. Demand size based fragmentation metric (DemFRAG)

By establishing and releasing connections dynamically, the spectrum finds free FSs called fragmented places that are not suitable to be allocated anymore, so the resource utilization reduces greatly. Hence, by having some metrics in defining fragmentation, we can establish a connection in a correct place through paths and enhance the resource utilization.

When the DAT technique is used, the number of FSs is allocated based on the path length, thus the number of necessary FSs will vary on different paths, since they have various length. For a more accurate evaluation of the spectrum fragmentation, for each path, the free blocks that can be allocated to the request and also those that cannot, are specified based on the required FSs on that path according to its length, and then the suitability of path for establishing the request is examined.

Suppose that there are n free frequency blocks on a path and the size of demand between the source and destination node is FS_{num} (required frequency slots). As discussed, the required FS_{num} will be different for each path depending on its length. We will take this into account to calculate the value of fragmentation on a path more accurately. For the path P and the required FS_{num}^P slots on this path, the demand size based fragmentation metric (DemFRAG) is calculated by Eq. (8):

$$DemFRAG(P, FS_{num}^P) = \frac{\sum_{j=1}^n dif(size(block_j^P), FS_{num}^P)}{\sum_{j=1}^n size(block_j^P)} \quad (8)$$

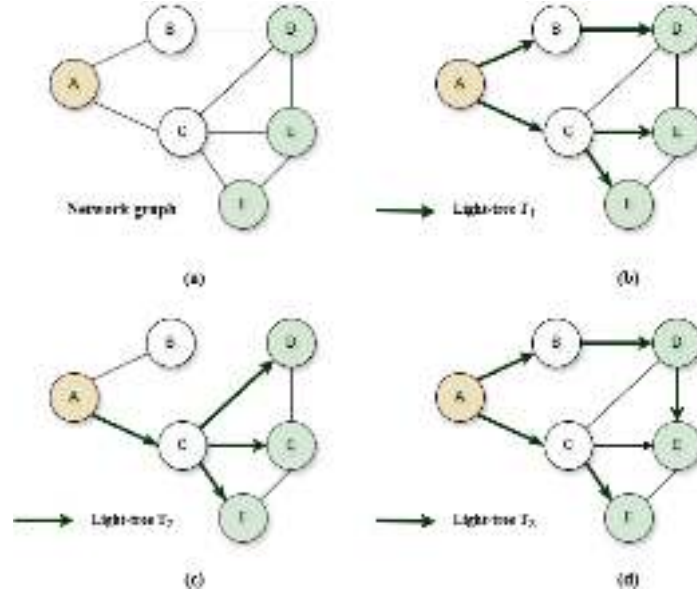


Fig. 1. An example network graph and various light-trees for a multicast request from node A to destination nodes $\{D, E, F\}$.

For each free frequency block $block_j^P$ on path P , we compute the difference between size of the block and the required FS_{num}^P slots on this path as follows:

$$dif(size(block_j^P), FS_{num}^P) = size(block_j^P) - FS_{num}^P \quad (9)$$

The dif function returns a positive or zero value for the blocks with suitable size for assigning to the request and a negative value for inappropriate ones. The lower value of the DemFRAG metric indicates more fragmentation of the spectrum on a path.

The Algorithm 1 describes the calculation steps of the DemFRAG metric for path P . To compute the fragmentation value in a path, the intersection of the statuses of the slots with the same index on all links along the path must be considered. In line 1, algorithm finds all free frequency blocks on path P . If at least one free frequency block exists on P , for each free block $block_j^P$, the size S_j^P and the difference dif_j^P between the size of the block and required frequency slots FS_{num}^P are calculated. If there is no free frequency block on P , the DemFRAG is set with the value $-FS_{max}$ in line 14. The FS_{max} is the maximum number of frequency slots on each link of the path.

To find all free frequency blocks on a path, the algorithm must check the status of all slots along the path, thus the complexity of line 1 is $O(FS_{max})$. Considering at most n free frequency blocks on a path, the complexity of lines 5 to 16 is $O(n) + O(1)$. Therefore, the overall complexity of calculation of the DemFRAG metric for a path is $O(FS_{max}) + O(n) + O(1) = O(FS_{max})$.

To calculate the fragmentation value in a light-tree, the intersection of the statuses of the slots with the same index on all links along the tree must be considered. Eqs. (8) and (9) can also be rewritten for a light-tree. In this case, the required number of frequency slots is calculated based on the diameter of the tree. For the light-tree T and the required FS_{num}^T slots on that, the DemFRAG is calculated by Eqs. (10) and (11):

$$DemFRAG(T, FS_{num}^T) = \frac{\sum_{j=1}^n dif(size(block_j^T), FS_{num}^T)}{\sum_{j=1}^n size(block_j^T)} \quad (10)$$

$$dif(size(block_j^T), FS_{num}^T) = size(block_j^T) - FS_{num}^T \quad (11)$$

The lower value of the DemFRAG metric indicates more fragmentation of the spectrum on a light-tree. In Section 4.1.1, we give an example to show how we can calculate the DemFRAG metric for a path or light-tree based on the required frequency slots (FS_{num}).

Algorithm 1: DemFRAG(P, FS_{num}^P)

Input: Spectrum occupation status of path P and number of required frequency slots FS_{num}^P on P

Output: Value of the DemFRAG metric for path P

```

1 Find all free frequency blocks on  $P$ 
2 if at least one free frequency block exists on  $P$  then
3    $S_{total}^P = 0$ 
4    $dif_{total}^P = 0$ 
5   for each free frequency block  $block_j^P$  on  $P$  do
6     Compute the size of  $block_j^P$  as  $S_j^P$ 
7     Compute the difference between  $S_j^P$  and the required
       frequency slots  $FS_{num}^P$  on  $P$  by Eq. (9) as  $dif_j^P$ 
8      $S_{total}^P = S_{total}^P + S_j^P$ 
9      $dif_{total}^P = dif_{total}^P + dif_j^P$ 
10  end
11  Compute the value of DemFRAG for  $P$  by Eq. (8)
12 end
13 else
14   DemFRAG =  $-FS_{max}$ 
15 end
16 return DemFRAG
```

4.1.1. Example

As an example, consider a request from node A to node E in the graph of Fig. 2 with two paths $P_1 = \{A \rightarrow B \rightarrow D \rightarrow E\}$ and $P_2 = \{A \rightarrow C \rightarrow D \rightarrow E\}$. Suppose that according to the amount of required bandwidth for this request, we need 3 frequency slots on P_1 and P_2 based on the length of these paths. P_1 consists of A – B, B – D, and D – E links, and P_2 includes A – C, C – D, and D – E links. The free and occupied frequency slots on each path and its links are shown in Fig. 2. In path P_1 , there are 2 frequency blocks with sizes 4 and 3 slots. So for this path, the DemFRAG can be calculated as follow:

$$DemFRAG(P_1, 3) = \frac{(4 - 3) + (3 - 3)}{7} = 0.143$$

There are 3 frequency blocks with sizes 2, 2, and 1 slots on path P_2 and the DemFRAG for this path can be calculated as follow:

$$DemFRAG(P_2, 3) = \frac{(2 - 3) + (2 - 3) + (1 - 3)}{5} = -0.8$$

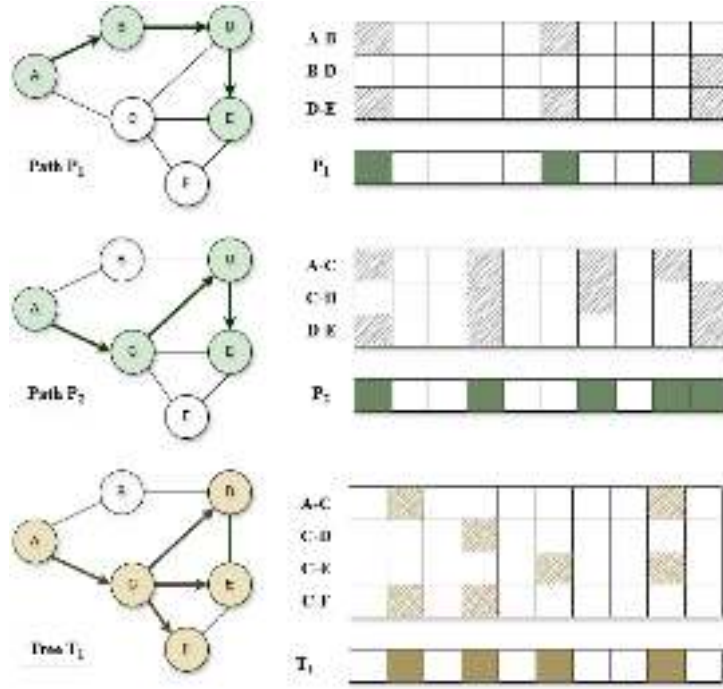


Fig. 2. An example of calculation of the DemFRAG metric for paths P_1 , P_2 and tree T_1 .

The value of $DemFRAG$ for P_2 is lower than P_1 because P_2 is more fragmented than P_1 . The P_1 is the least fragmented path among these two paths and is more suitable for setting up the request.

Consider the light-tree T_1 for a multicast request from source node A to destination nodes $\{D, E, F\}$. Suppose that according to the amount of required bandwidth for this request, we need 2 frequency slots on T_1 based on its diameter. The tree T_1 consists of $A - C$, $C - D$, $C - E$, and $C - F$ links. There are 5 frequency blocks with sizes 1, 1, 1, 2, and 1 slots on links of T_1 , thus we calculate the $DemFRAG$ metric as follow:

$$DemFRAG(T_1, 2) = \frac{(1-2) + (1-2) + (1-2) + (2-2) + (1-2)}{6} = -0.67$$

The tree T_1 has only one suitable block for setting up this request and its $DemFRAG$ value is lower than zero, thus it is relatively fragmented.

4.2. Network model

We consider core-networks architecture, so that each node generates its own traffic. The network is considered as a graph $G(V, E)$ where V is the set of nodes and E is the set of bidirectional links used to connect different nodes. We assume that all nodes in the network are multicast-capable. A multicast request is presented as $mR_i(s_i, D_i, b_i, t_i)$ where s_i is the source node, D_i is the set of destination nodes, b_i is the required bandwidth and t_i is the holding time of the multicast request mR_i . Requests can arrive at the network at any time.

The notations and variables used in the proposed algorithms are mentioned in Table 4.

4.3. The LFPT-MRMSA algorithm

The Least Fragmented Path based Tree Multicast Routing, Modulation level and Spectrum Assignment (LFPT-MRMSA) algorithm is presented in Algorithm 3. The network graph G , the multicast request $mR_i(s_i, D_i, b_i, t_i)$, and the list of K -shortest paths between each pair of nodes in G are the inputs of the algorithm. The construction of the multicast light-tree for the request mR_i is carried out by using the shortest candidate paths between the source node and destination nodes (shortest path tree). We denote the list of shortest paths from

source node s_i to destination node d by $Path^d$, and $Path^{D_i}$ is the list of $Path^d$ for destination set D_i .

In lines 1 to 6, for each node d in the destination set D_i and for each path p in the $Path^d$, the amount of spectrum fragmentation $FragMetric_p^d$ is calculated by using the DemFRAG metric and then $Path^d$ is sorted based on the calculated $FragMetric_p^d$ values in descending order.

At the next step, the $Build - LFPT(s_i, D_i, Path^{D_i})$ procedure illustrated in Algorithm 2 is called to construct the multicast tree for the request mR_i based on the least fragmented paths. In this procedure, for each d in the set D_i , the shortest path that has the least value of fragmentation has higher priority to be selected and added to the multicast tree.

In line 8 of Algorithm 3, the modulation level is selected according to the diameter of the constructed tree T_i and the required frequency slots $FS_{num}^{T_i}$ on this tree is calculated. If there are free frequency blocks with at least $FS_{num}^{T_i}$ slots on T_i , the first-fit policy is used to assign the block to the request by observing the contiguity, continuity, and non-overlapping constraints, and the multicast request mR_i is setup. Otherwise, it will be blocked. In this algorithm, if the multicast request mR_i is established, the *Blocked* variable is set to 0; otherwise, it will be 1 which means that the request has been blocked.

4.3.1. Complexity of the LFPT-MRMSA algorithm

In the following, we analyze the computational time complexity of the LFPT-MRMSA algorithm in Algorithm 3. First, we calculate the complexity of the $Build - LFPT()$ procedure presented in Algorithm 2. The complexity of lines 2 and 3 are $O(K)$ and $O(|D_i|)$, respectively. The for loop in line 5 is repeated $O(|E|)$ times in the worst case. The complexity of checking that whether T_i is tree or not is $O(|V| + |E|)$ in line 9. The overall complexity of the $Build - LFPT()$ function is:

$$O\left(K \times (|D_i| \times |E| + (|V| + |E|))\right) = O\left(K \times |D_i| \times |E| + K \times |V| + K \times |E|\right) = O\left(K \times |D_i| \times |E|\right) \quad (12)$$

In Algorithm 3, the complexity of lines 1 to 6 is $O(|D_i| \times (K \times FS_{max} + K \times \log(K))) = O(|D_i| \times K \times FS_{max})$. The $K \times \log(K)$ is the

Table 4
Notations and variables.

Variable	Description
b_i	The required bandwidth of the multicast request i
$Blocked$	A binary variable that indicates blocking status of a multicast request
BP	The blocking probability
BBP	The bandwidth blocking probability
D_i	The set of destination nodes of the multicast request i
E	The set of links in the network
$FragMetric_p^d$	The fragmentation value of the path p from source node s_i to destination node d
FS_{num}^P	The required frequency slots on path P
FS_{num}^T	The required frequency slots on tree T
FS_{max}	The maximum number of frequency slots on each link of G
G	The network graph
K	The number of shortest paths between node pairs
m	A number that indicates the selected modulation format
mR_i	The multicast request i
N_G	The number of guard band slots
$Path^d$	The list of shortest paths from source node s_i to destination node d
$Path^{D_i}$	The list of $Path^d$ for destination set D_i
s_i	The source node of the multicast request i
t_i	The holding time of the multicast request i
V	The set of nodes in the network
Y_{slot}	The width of one frequency slot

Algorithm 2: *Build – LFPT*($s_i, D_i, Path^{D_i}$)

Input: Source node s_i , set of destination nodes D_i , and sorted list of paths $Path^{D_i}$

Output: Multicast light-tree T_i

```

1  $T_i = \emptyset$ 
2 for  $r = 1$  to  $K$  do
3   for each  $d$  in  $D_i$  do
4     Get  $r$ th path from  $s_i$  to  $d$  from  $Path^d$  as  $path_r^d$ 
5     for each edge  $e$  on  $path_r^d$  do
6       Add  $e$  to  $T_i$ 
7     end
8   end
9   if  $isTree(T_i)$  then
10    return  $T_i$ 
11  end
12 end

```

complexity of sorting $Path^d$ in descending order in line 5. Selecting the modulation level according to the diameter of tree has $O(|E|)$ complexity in worst case because to calculate the diameter of tree, we have to obtain the total length of links along the longest path in tree. Finding free frequency blocks has $O(n)$ complexity if there are at most n free blocks on T_i . The complexity of line 10 for assigning slots of frequency block on all links of T_i is $O(FS_{num}^T \times |E|)$ in the worst case. The lines 12, 15 and 17 have $O(1)$ complexity, thus the overall complexity of the LFPT-MRMSA algorithm is as follow:

$$\begin{aligned}
& O(|D_i| \times K \times FS_{max} + (K \times |D_i| \times |E|) + |E| + n + FS_{num}^T \times |E|) \\
& = O(|D_i| \times K \times (FS_{max} + |E|)) \quad (13)
\end{aligned}$$

4.4. The OLFT-MRMSA algorithm

The Optimal Least Fragmented Tree Multicast Routing, Modulation level and Spectrum Assignment (OLFT-MRMSA) algorithm is presented in Algorithm 5. The inputs of algorithm are the network graph G , the multicast request $mR_i(s_i, D_i, b_i, t_i)$, and the list of K-shortest paths between each pair of nodes in G . We denote the list of shortest paths from source node s_i to destination node d by $Path^d$ and $Path^{D_i}$ is the list of $Path^d$ for destination set D_i . The *Build – OLFT*($s_i, D_i, Path^{D_i}$) procedure presented in Algorithm 4 is called in line 1 to construct the

Algorithm 3: LFPT-MRMSA

Input: Network graph G , multicast request $mR_i(s_i, D_i, b_i, t_i)$, and list of K-shortest paths between each pairs of nodes in G

Output: Status of the multicast request mR_i

```

1 for each  $d$  in  $D_i$  do
2   for each  $p$  in  $Path^d$  do
3     Compute the fragmentation value of  $p$  as  $FragMetric_p^d$ 
      by using the DemFRAG metric
4   end
5   Sort  $Path^d$  according to the values of  $FragMetric_p^d$  in
      descending order
6 end
7  $T_i = Build - LFPT(s_i, D_i, Path^{D_i})$ 
8 Select the modulation level according to the diameter of the
   multicast tree  $T_i$  and calculate  $FS_{num}^T$  by using Eq. (7)
9 if free frequency blocks with at least  $FS_{num}^T$  slots are available on
    $T_i$  then
10  Use the first-fit policy to assign the block
11  Setup the multicast request  $mR_i$ 
12   $Blocked = 0$ 
13 end
14 else
15   $Blocked = 1$ 
16 end
17 return  $Blocked$ 

```

multicast tree for request mR_i . In this procedure, there are N_t iterations, and in each one of them, a random light-tree is constructed. At each iteration $iter$, for each d in the set D_i , one of the shortest paths from s_i to d is selected randomly from the list $Path^d$ and added to tree. At the next step, the fragmentation value of constructed tree T_{iter} is computed as $Cost_{iter}$ by using the DemFRAG metric and compared with $Cost_{opt}$ of the best so far created tree T_{opt} . If $Cost_{iter}$ is better than $Cost_{opt}$, the $Cost_{opt}$ and T_{opt} will be updated. The *Build – OLFT*($s_i, D_i, Path^{D_i}$) returns best multicast light-tree among N_t various constructed trees. By considering a large value for N_t , the optimal tree that has the least fragmentation value can be found.

Similar to the LFPT-MRMSA algorithm, in line 2 of Algorithm 5, the modulation level is selected according to the diameter of the constructed optimal light-tree T_i and the required frequency slots FS_{num}^T on this tree is calculated. If there are free frequency blocks with at least

Algorithm 4: *Build – OLFT*($s_i, D_i, Path^{D_i}$)

Input: Source node s_i , set of destination nodes D_i , and list of paths $Path^{D_i}$

Output: Multicast light-tree T_{opt}

```

1  $T_{iter} = \emptyset$ 
2  $T_{opt} = \emptyset$ 
3  $Cost_{opt} = -\infty$ 
4 for  $iter = 1$  to  $N_t$  do
5   for each  $d$  in  $D_i$  do
6     Randomly select a path from  $s_i$  to  $d$  from  $Path^d$  as
        $path_r^d$ 
7     for each edge  $e$  on  $path_r^d$  do
8       Add  $e$  to  $T_{iter}$ 
9     end
10  end
11  if  $isTree(T_{iter})$  then
12    Compute the fragmentation value of tree  $T_{iter}$  as  $Cost_{iter}$ 
      by using the DemFRAG metric
13    if  $Cost_{iter}$  is better than  $Cost_{opt}$  then
14       $Cost_{opt} = Cost_{iter}$ 
15       $T_{opt} = T_{iter}$ 
16    end
17  end
18 end
19 return  $T_{opt}$ 

```

Algorithm 5: OLFT-MRMSA

Input: Network graph G , multicast request $mR_i(s_i, D_i, b_i, t_i)$, and list of K-shortest paths between each pairs of nodes in G

Output: Status of the multicast request mR_i

```

1  $T_i = Build - OLFT(s_i, D_i, Path^{D_i})$ 
2 Select the modulation level according to the diameter of the
  multicast tree  $T_i$  and calculate  $FS_{num}^{T_i}$  by using Eq. (7)
3 if free frequency blocks with at least  $FS_{num}^{T_i}$  slots are available on
   $T_i$  then
4   Use the first-fit policy to assign the block
5   Setup the multicast request  $mR_i$ 
6    $Blocked = 0$ 
7 end
8 else
9    $Blocked = 1$ 
10 end
11 return  $Blocked$ 

```

$FS_{num}^{T_i}$ slots on T_i , the first-fit policy is used to assign the block to the request by observing the contiguity, continuity, and non-overlapping constraints, and the multicast request mR_i is setup. Otherwise, it will be blocked. In this algorithm, if the multicast request mR_i is established, the *Blocked* variable is set to 0, and otherwise it will be 1, which means that the request has been blocked.

4.4.1. Complexity of the OLFT-MRMSA algorithm

In the following, we analyze the computational time complexity of the OLFT-MRMSA algorithm in Algorithm 5. First, we calculate the complexity of the *Build – OLFT*() procedure presented in Algorithm 4. The complexity of lines 5 to 10 are $O(|D_i| \times |E|)$. The lines 11 to 16 have $O((|V| + |E|) + FS_{max})$ time complexity. The overall complexity of the *Build – OLFT*() procedure is:

$$O\left(N_t \times \left(|D_i| \times |E| + (|V| + |E|) + FS_{max}\right)\right) = O\left(N_t \times \left(|D_i| \times |E| + FS_{max}\right)\right) \quad (14)$$

In the Algorithm 5, selecting the modulation level according to the diameter of tree in line 2 has $O(|E|)$ complexity. Finding free frequency blocks in line 3 has $O(n)$ complexity if at most n free blocks are available on T_i . The complexity of line 4 for assigning slots of frequency block on all links of T_i is $O(FS_{num}^{T_i} \times |E|)$ in the worst case. The lines 5, 6, 9 and 11 have $O(1)$ complexity, thus the overall complexity of the OLFT-MRMSA algorithm is as follows:

$$O\left(N_t \times \left(|D_i| \times |E| + FS_{max}\right) + |E| + n + FS_{num}^{T_i} \times |E|\right) = O\left(N_t \times \left(|D_i| \times |E| + FS_{max}\right) + FS_{num}^{T_i} \times |E|\right) \quad (15)$$

5. Simulation results

To evaluate the performance of the proposed fragmentation-aware MRMSA algorithms with novel DemFRAG metric, we use the NSFNET and JPN12 network topologies that are depicted in Figs. 3 and 4, respectively. The source and destinations of multicast requests are randomly and uniformly distributed among the network nodes. Requests enter the network with a Poisson distribution, and the inter-arrival time between them follows an exponential distribution with mean of λ , the holding time of requests follows an exponential distribution with mean of μ . The total number of multicast requests is 10,000 and for each request, 3, 4 or 5 distinct destinations are randomly selected with uniform distribution. The network load is assumed to be between 1000 to 5000 Erlang with the step of 1000 Erlang, and the required bandwidth of incoming requests is 300, 400, 500, 700, and 900 Gbps. We have considered the number of shortest paths between each pair of source and destination nodes as 5 paths. Confidence interval is considered 95% in the simulations and confidence interval bars are depicted in the figures. The number of frequency slots on each link is 320 and the guard band occupies 1 frequency slot. In the simulations, μ is set to 10 s and λ is calculated based on the assumed network load in Erlang. The simulation results have been repeated 15 times for each value of λ and the values of Blocking Probability (BP) (Eq. (16)) and Bandwidth Blocking Probability (BBP) (Eq. (17)) have been compared with other fragmentation-aware algorithms.

$$BP = \frac{\text{Number of blocked multicast requests}}{\text{Number of total multicast requests}} \quad (16)$$

$$BBP = \frac{\text{Bandwidth of blocked multicast requests}}{\text{Bandwidth of all multicast requests}} \quad (17)$$

Simulation parameters are stated in Table 5. In the simulations, we compare the performance of the proposed LFPT-MRMSA and OLFT-MRMSA algorithms considering the EF [7], FMM [10], NPFR [8], Golden [9], Fc [40], and DemFRAG fragmentation metrics:

- **LFPT+EF** - The LFPT-MRMSA algorithm that uses the EF metric
- **LFPT+FMM** - The LFPT-MRMSA algorithm that uses the FMM metric
- **LFPT+NPFR** - The LFPT-MRMSA algorithm that uses the NPFR metric
- **LFPT+Fc** - The LFPT-MRMSA algorithm that uses the Fc metric
- **LFPT+DemFRAG** - The LFPT-MRMSA algorithm that uses the DemFRAG metric
- **OLFT+EF** - The OLFT-MRMSA algorithm that uses the EF metric
- **OLFT+FMM** - The OLFT-MRMSA algorithm that uses the FMM metric
- **OLFT+NPFR** - The OLFT-MRMSA algorithm that uses the NPFR metric
- **OLFT+Fc** - The OLFT-MRMSA algorithm that uses the Fc metric
- **OLFT+DemFRAG** - The OLFT-MRMSA algorithm that uses the DemFRAG metric

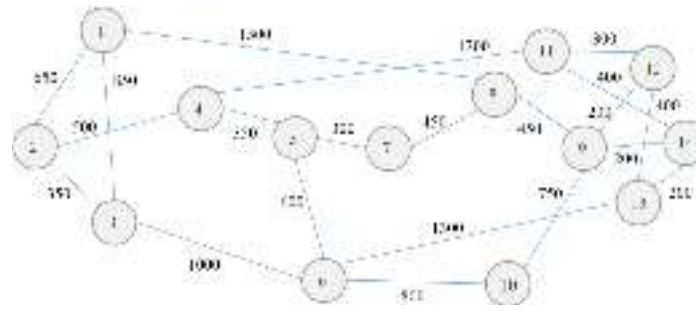


Fig. 3. NSFNET topology.

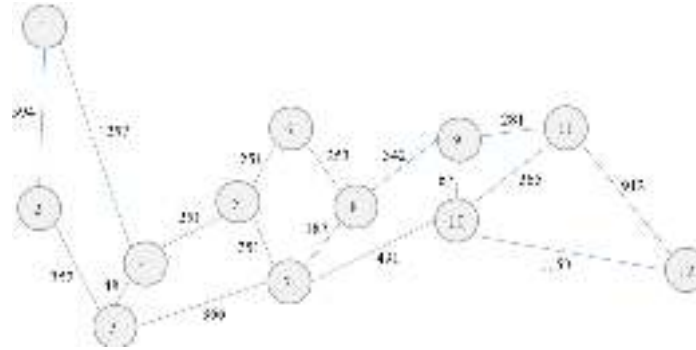


Fig. 4. JPN12 topology.

Table 5

Simulation parameters.

Parameter	Value
Number of nodes	14 (NSFNET), 12 (JPN12)
Number of bidirectional links	21 (NSFNET), 17 (JPN12)
Number of frequency slots per link	320
Each frequency slot spectrum width (GHz)	12.5
Link capacity (THz)	4
Number of guard-band frequency slots	1
Number of multicast requests	10 000
Random number of destinations	3, 4, 5
Traffic type (Gbps)	300, 400, 500, 700, 900
Mean service time	10
Network load (Erlang)	1000, 2000, 3000, 4000, 5000

5.1. NSFNET network

The NSFNET network has 14 nodes and 21 bidirectional links. Results of the LFPT-MRMSA and OLFPT-MRMSA algorithms in this network are presented in the next subsections.

5.1.1. Results of the LFPT-MRMSA algorithm

Simulation results of the LFPT-MRMSA algorithm under NSFNET network topology are shown in Figs. 5–9.

For 300 Gbps traffic, as depicted in Fig. 5(a), at the load of 1000 Erlang, all algorithms have almost similar BP and BBP values but when the network load exceeds 2000 Erlang, the BP of LFPT+DemFRAG is lower than all other algorithms and its better performance is obvious. From Fig. 5(b), the LFPT-MRMSA algorithm with the DemFRAG metric has the least BBP value at the network loads greater than 2000 Erlang. Therefore, more multicast requests can be set up by using this metric. The LFPT+EF, LFPT+FMM and LFPT+NPFR algorithms have the most BP and BBP values at all network loads. The LFPT+Golden and LFPT+Fc have lower BP and BBP values compared to other algorithms except the LFPT+DemFRAG algorithm.

For 400 Gbps traffic, as depicted in Fig. 6(a), at all network loads, the BP of LFPT+DemFRAG is lower than all other algorithms and it

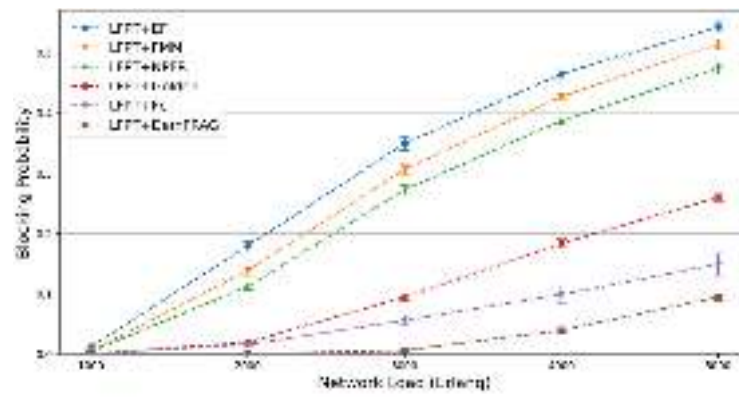
has better performance. At network loads of 2000 to 5000 Erlang, the superiority of the LFPT+DemFRAG algorithm is more obvious compared to others. From Fig. 6(b), the LFPT-MRMSA algorithm with the DemFRAG metric has the least BBP value at the network loads greater than 2000 Erlang. Therefore, more multicast requests can be setup in this algorithm. The LFPT+EF algorithm has the most BP and BBP values at all network loads.

For 500 Gbps traffic, as depicted in Figs. 7(a) and 7(b), at the load of 1000 Erlang, the BP and BBP values of the LFPT+DemFRAG algorithm are almost zero. When the network load exceeds 2000 Erlang, the BP value of LFPT+DemFRAG is lower than all other algorithms. From Fig. 7(b), the LFPT-MRMSA algorithm with the DemFRAG metric has the least BBP value at network load of 2000 Erlang and it has had a significant decrease in BBP value compared to other algorithms. The LFPT+EF algorithm has the most BP and BBP values at all network loads. The LFPT+FMM and LFPT+NPFR algorithms have relatively the same performance at 500 Gbps traffic requests. The LFPT+DemFRAG algorithm has the least BP and BBP values at all network loads.

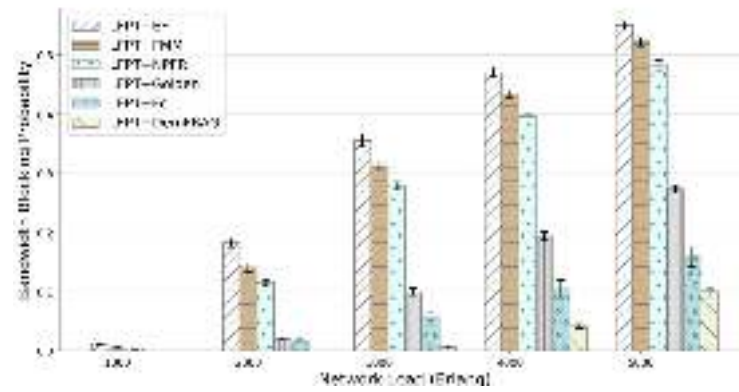
For 700 Gbps traffic, as depicted in Figs. 8(a) and 8(b), the BP and BBP values of the LFPT+DemFRAG algorithm are lower than all other algorithms at all network loads. The LFPT+EF algorithm has the most BP and BBP values at all network loads. The LFPT+NPFR has been a little better than the LFPT+FMM algorithm. At network loads of 1000 and 2000 Erlang, the BP and BBP values of LFPT+Golden are lower than LFPT+Fc but when the network load exceeds 3000 Erlang, the LFPT+Fc algorithm has lower BP and BBP values. The LFPT+DemFRAG algorithm has the least BP and BBP values at all network loads among all algorithms.

When we increase the traffic requests to 900 Gbps, the BP and BBP values at all network loads increase. As depicted in Figs. 9(a) and 9(b), the LFPT+DemFRAG algorithm has the least BP and BBP values at all network loads. The LFPT+FMM and LFPT+NPFR algorithms have relatively the same performance at 900 Gbps traffic requests and the highest BP and BBP values are for the LFPT+EF algorithm.

Therefore, we can conclude that for all types of bandwidth requests in the NSFNET network topology, the LFPT-MRMSA algorithm with the

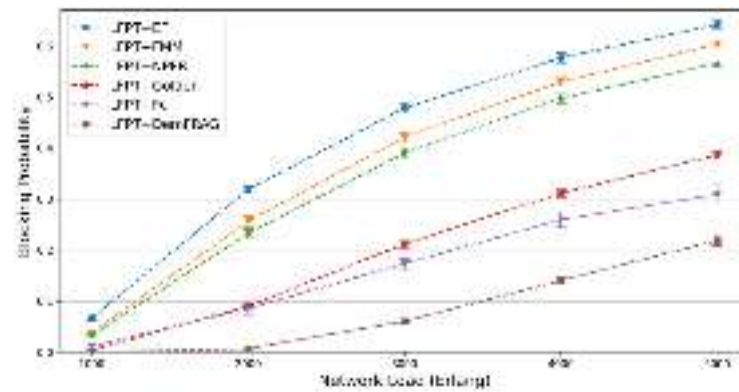


(a) BP

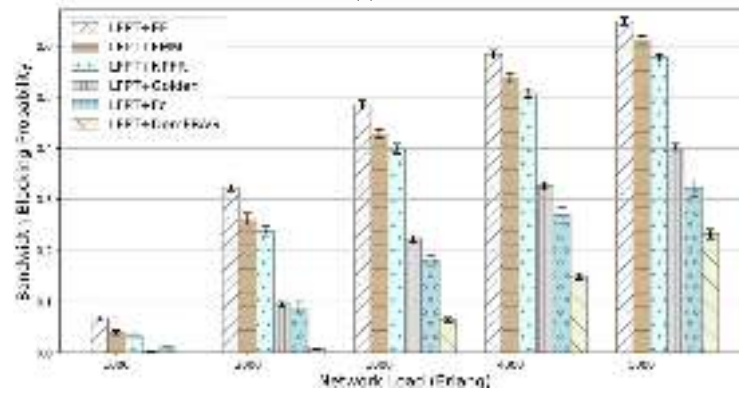


(b) BBP

Fig. 5. Simulation results of LFPT-MRMSA under NSFNET topology at 300 Gbps traffic requests.

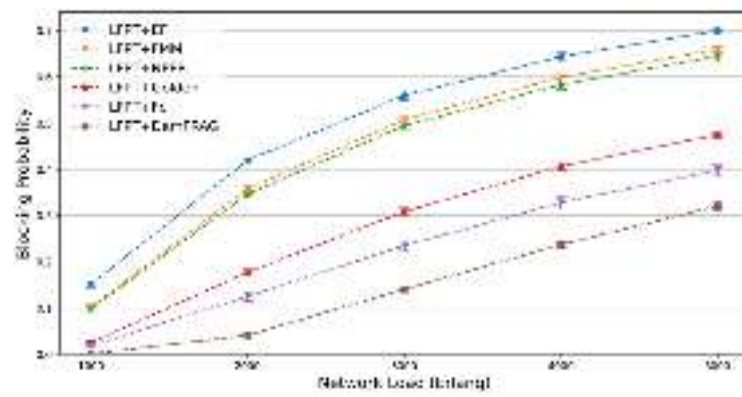


(a) BP

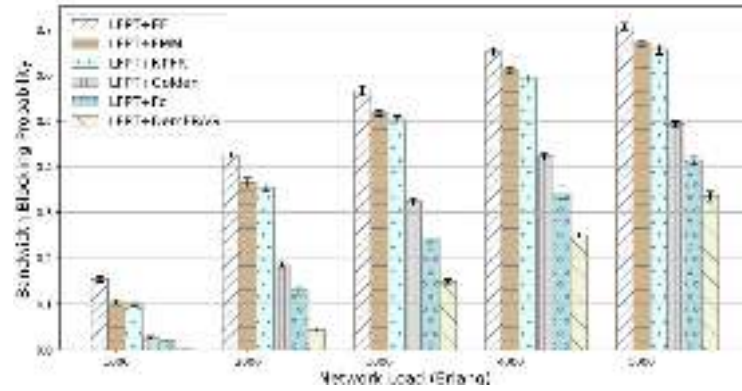


(b) BBP

Fig. 6. Simulation results of LFPT-MRMSA under NSFNET topology at 400 Gbps traffic requests.

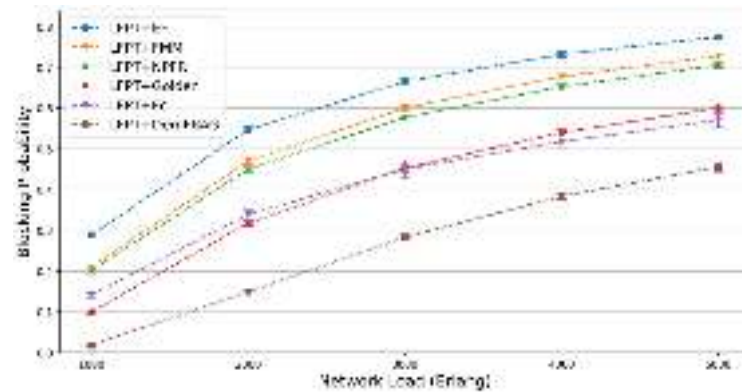


(a) BP

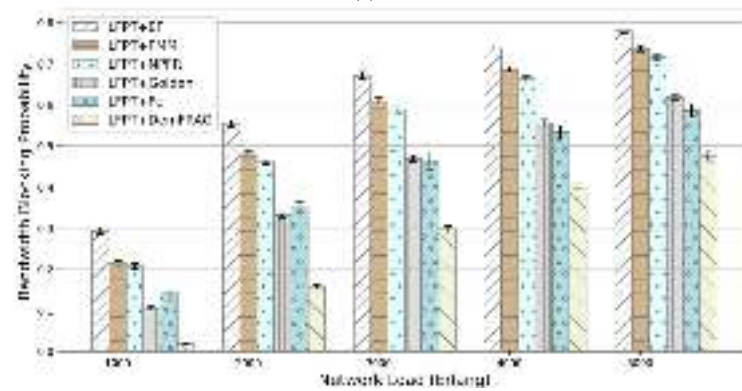


(b) BBP

Fig. 7. Simulation results of LFPT-MRMSA under NSFNET topology at 500 Gbps traffic requests.



(a) BP



(b) BBP

Fig. 8. Simulation results of LFPT-MRMSA under NSFNET topology at 700 Gbps traffic requests.

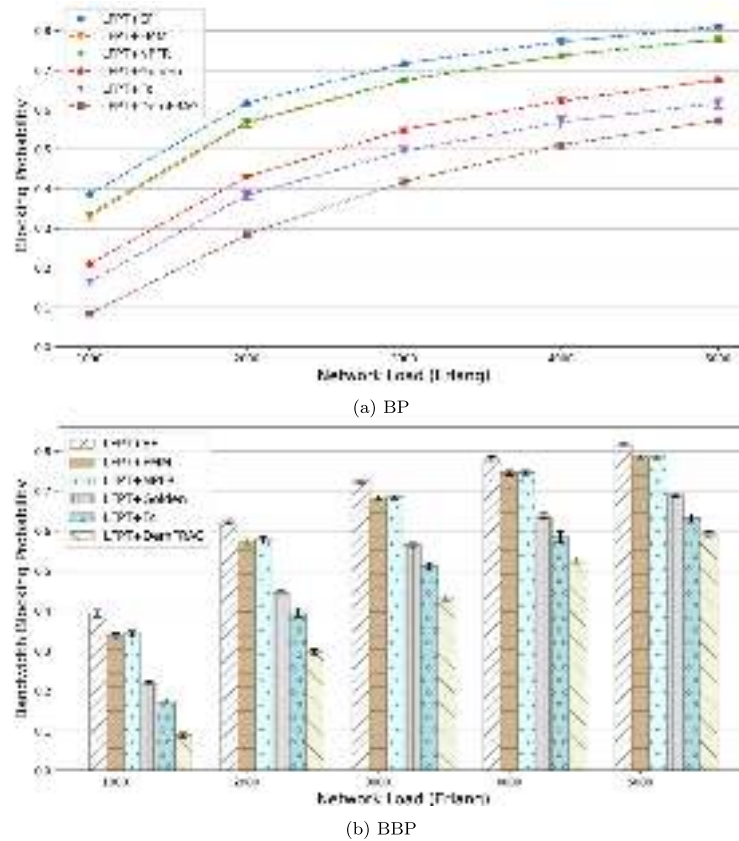


Fig. 9. Simulation results of LFPT-MRMSA under NSFNET topology at 900 Gbps traffic requests.

DemFRAG metric improves the efficiency of multicasting by reducing BP and BBP, and compared to the LFPT-MRMSA algorithm that uses other fragmentation metrics, it obtains better performance.

5.1.2. Results of the OLFT-MRMSA algorithm

Simulation results of the OLFT-MRMSA algorithm under NSFNET network topology are shown in the Figs. 10–14. In simulations, we set the N_t to 30, thus the least fragmented tree is selected out of 30 different constructed trees.

For 300 Gbps traffic, as depicted in Fig. 10(a), BP of the OLFT+FMM algorithm is higher than others. The OLFT+EF and OLFT+NPFR algorithms have similar BP values. The OLFT+Fc and OLFT+DemFRAG algorithms have lower BP values between all others. The least BP value is for the OLFT-MRMSA algorithm with the DemFRAG metric at network loads greater than 2000 Erlang. From Fig. 10(b), at network loads between 1000 and 2000 Erlangs, the BBP values of the OLFT+Fc and OLFT+DemFRAG algorithms are almost zero. At network loads of 3000, 4000, and 5000 Erlang, our proposed OLFT+DemFRAG algorithm has the least BBP value among all other algorithms.

For 400 Gbps traffic, as depicted in Figs. 11(a) and 11(b), the least BP and BBP values are for our OLFT-MRMSA algorithm with the DemFRAG metric at all network loads. The BP and BBP values of the OLFT+FMM algorithm are higher than other algorithms. The OLFT+EF and OLFT+NPFR algorithms have relatively similar BP and BBP values. The OLFT+Fc and OLFT+DemFRAG algorithms have lower BP values between all others. At network load of 1000 Erlang, the BP and BBP values of the OLFT+Fc and OLFT+DemFRAG algorithms are almost zero.

For 500 Gbps traffic, as depicted in Fig. 12(a), the BP values of OLFT+FMM, OLFT+EF and OLFT+NPFR algorithms are relatively similar and higher than the OLFT+Golden, OLFT+Fc and OLFT+DemFRAG algorithms. The OLFT+Fc and OLFT+DemFRAG algorithms have lower BP values between all others. The least BP value is for our

OLFT-MRMSA algorithm with the DemFRAG metric at network loads greater than 2000 Erlang. From Fig. 12(b), at network load of 1000 Erlang, the BBP values of the OLFT+Fc and OLFT+DemFRAG algorithms are almost zero. At network loads of 3000, 4000, and 5000 Erlang, OLFT+DemFRAG has the least BBP value among all other algorithms.

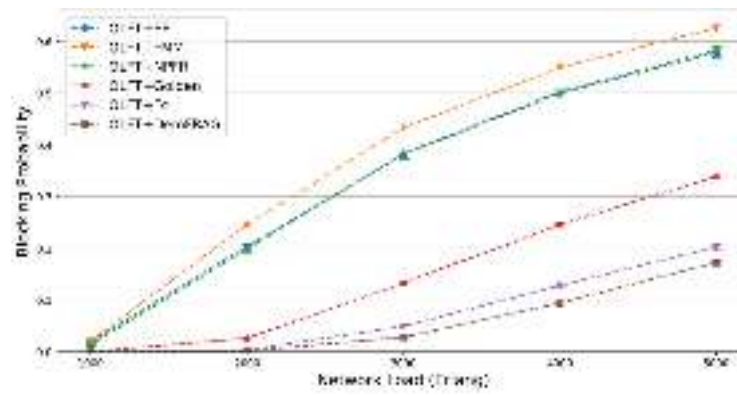
According to the simulation results at 700 Gbps traffic requests in Figs. 13(a) and 13(b), the values of BP and BBP for the OLFT+FMM and OLFT+EF algorithms are relatively similar and higher than others. The least BP and BBP values are for the OLFT-MRMSA algorithm with the DemFRAG metric at all network loads.

The simulation results at 900 Gbps traffic requests illustrated in Figs. 14(a) and 14(b). According to these figures, we can observe that at network loads of 4000 and 5000 Erlang, the OLFT+DemFRAG and OLFT+Fc algorithms have the least BP and BBP values. At network loads lower than 4000 Erlang, the OLFT+DemFRAG algorithm is better than OLFT+Fc in reducing the BP and BBP values. Results show that the highest BP and BBP values obtained when we use the EF, FMM and NPFR metrics in the OLFT-MRMSA algorithm.

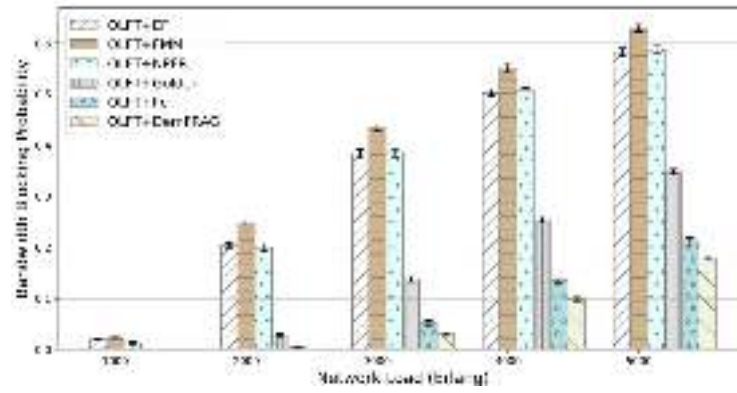
We can conclude that for all types of requested bandwidth in the NSFNET topology, the OLFT-MRMSA algorithm with the DemFRAG metric improves the efficiency of multicasting by reducing BP and BBP. By considering large values for the number of total constructed multicast trees N_t , we can get better results in the OLFT-MRMSA algorithm but the time complexity will be increased.

5.2. JPN12 network

The JPN12 network is a thinner and wider topology compared to the NSFNET. It has 12 nodes and 17 bidirectional links. Simulation results of the LFPT-MRMSA and OLFT-MRMSA algorithms in this network are discussed in the next subsections.

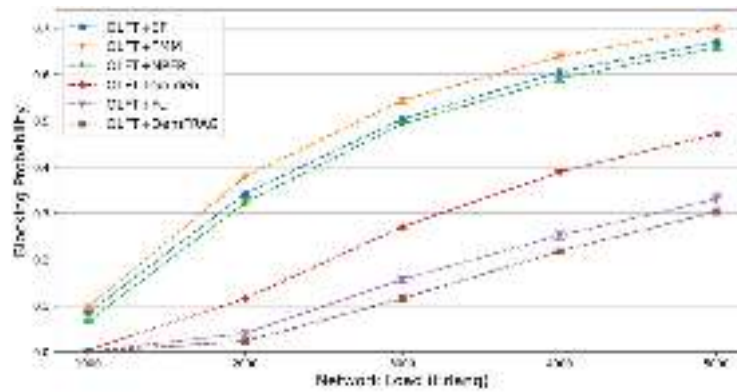


(a) BP

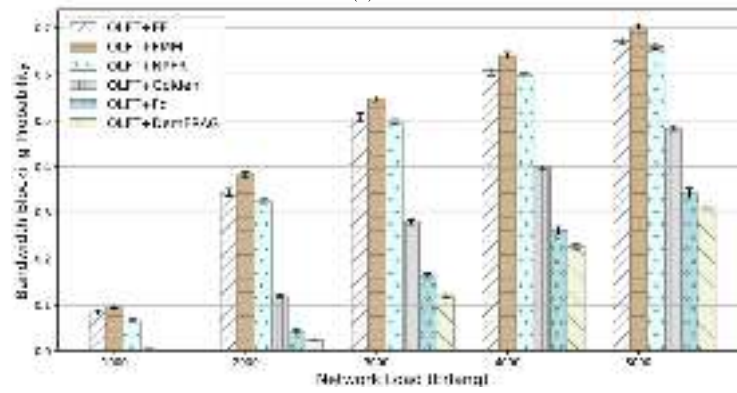


(b) BBP

Fig. 10. Simulation results of OLFT-MRMSA under NSFNET topology at 300 Gbps traffic requests.

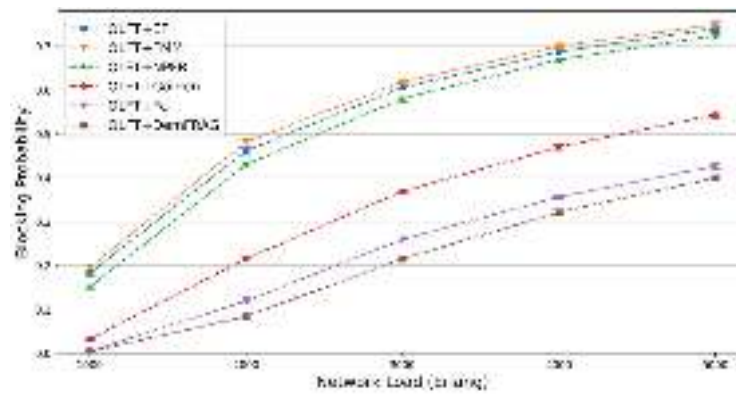


(a) BP

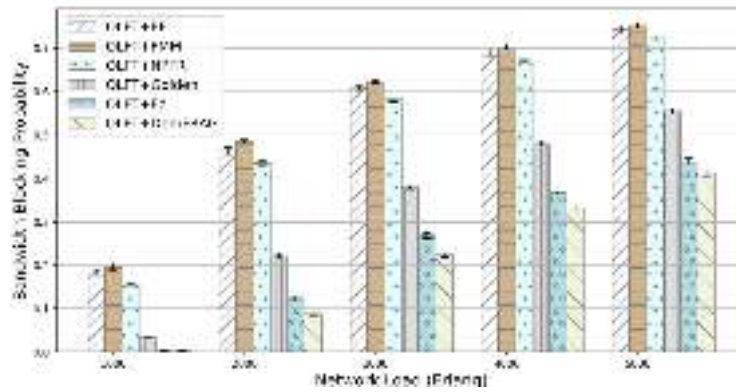


(b) BBP

Fig. 11. Simulation results of OLFT-MRMSA under NSFNET topology at 400 Gbps traffic requests.

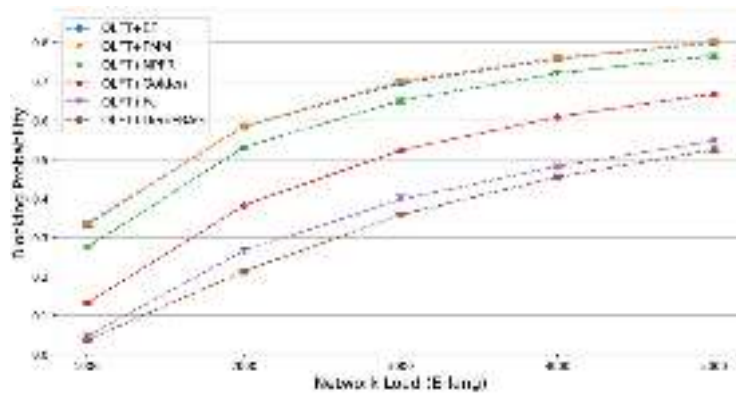


(a) BP

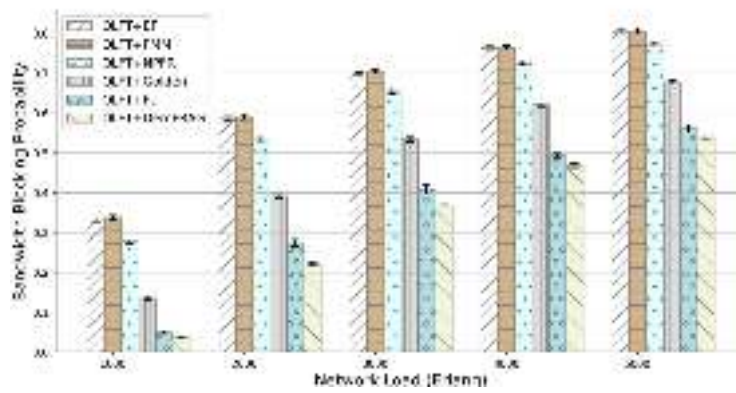


(b) BBP

Fig. 12. Simulation results of OLF-T-MRMSA under NSFNET topology at 500 Gbps traffic requests.



(a) BP



(b) BBP

Fig. 13. Simulation results of OLF-T-MRMSA under NSFNET topology at 700 Gbps traffic requests.

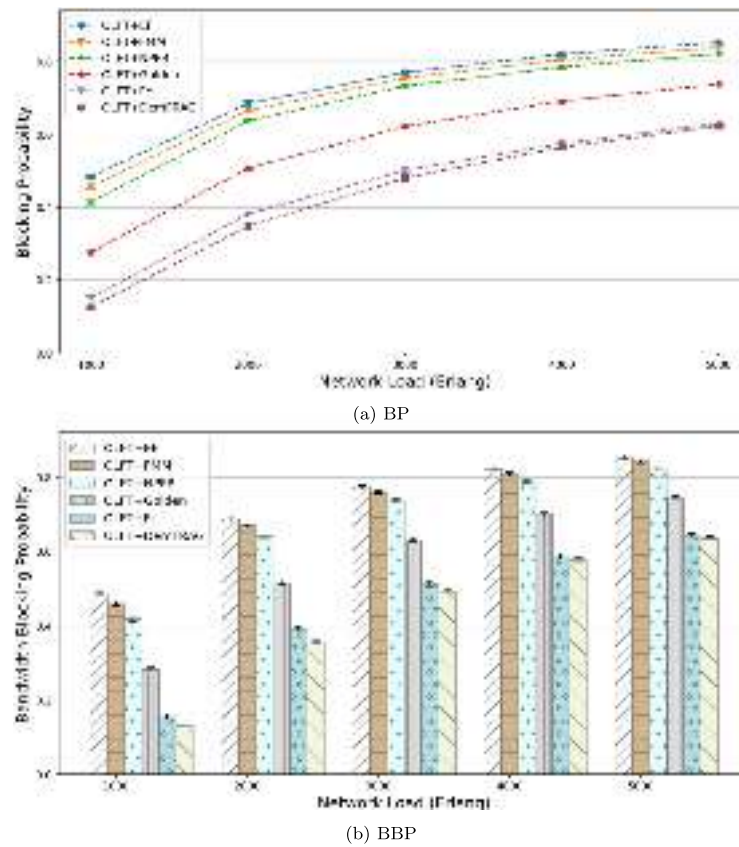


Fig. 14. Simulation results of OLFT-MRMSA under NSFNET topology at 900 Gbps traffic requests.

5.2.1. Results of the LFPT-MRMSA algorithm

Simulation results of the LFPT-MRMSA algorithm under JPN12 network topology are illustrated in Figs. 15–19 at traffic requests of 300, 400, 500, 700, and 900 Gbps.

Figs. 15(a) and 15(b) show the BP and BBP values at 300 Gbps traffic requests respectively. At the network load of 1000 Erlang, the BP and BBP values of all algorithms are almost zero. When the network load exceeds 3000 Erlang, the BP and BBP of the LFPT+EF, LFPT+FMM and LFPT+NPFR algorithms increase significantly. The LFPT+Golden and LFPT+Fc have relatively the same performance. The least BP and BBP values are for LFPT+DemFRAG at all network loads.

The results of algorithms in JPN12 at 400 Gbps (see Figs. 16(a) and 16(b)) are similar to 300 Gbps traffic requests. At the network load of 1000 Erlang, the BP and BBP values of all algorithms are near zero. The highest BP and BBP are for LFPT+EF and LFPT+FMM. The LFPT+DemFRAG has the best performance at all network loads.

For 500 Gbps traffic, as depicted in Figs. 17(a) and 17(b), the least BP and BBP values are for the LFPT-MRMSA algorithm with the DemFRAG metric at all network loads.

For 700 and 900 Gbps traffic requests, as depicted in Figs. 18–19, the BP and BBP in all algorithms increase significantly. The LFPT+EF, LFPT+FMM and LFPT+NPFR algorithms have higher BP and BBP values. The least BP and BBP values are for LFPT+DemFRAG at all network loads.

According to the results of simulation under the JPN12 network topology, we can conclude that for all types of requested bandwidth, the LFPT-MRMSA algorithm with the DemFRAG metric improves the efficiency of multicasting by reducing BP and BBP, and compared to the LFPT-MRMSA algorithm that uses other fragmentation metrics, it obtains better performance.

5.2.2. Results of the OLFT-MRMSA algorithm

Simulation results of the OLFT-MRMSA algorithm under JPN12 network topology are illustrated in Figs. 20–24. In simulations, we set the N_t to 30, thus the least fragmented tree is selected out of 30 different constructed trees.

Simulation results at 300 Gbps traffics are shown in Figs. 20(a) and 20(b). At the network load of 1000 Erlang, the BP and BBP values of all algorithms are almost zero. When the network load exceeds 2000 Erlang, the BP and BBP of the OLFT+EF, OLFT+FMM and OLFT+NPFR algorithms increase significantly. The highest BP and BBP values are for the OLFT+FMM algorithm. The performance of the OLFT+DemFRAG algorithm is slightly better than OLFT+Fc at 4000 and 5000 network loads.

According to simulation results at 400 Gbps traffic requests in Figs. 21(a) and 21(b), the highest BP and BBP values are for the OLFT+FMM algorithm at all network loads. The performance of OLFT+DemFRAG is slightly better than OLFT+Fc at the network load of 3000 to 5000 Erlang.

For 500 Gbps traffics, as illustrated in Figs. 22(a) and 22(b), the OLFT+Fc and OLFT+DemFRAG have relatively the same performance. The OLFT+FMM has the worst performance among all algorithms.

According to the simulation results at 700 Gbps traffic requests in Figs. 23(a) and 23(b), when the network load exceeds 2000 Erlang, the performance of the OLFT+DemFRAG algorithm is become better than OLFT+Fc. The highest BP and BBP values are for the OLFT+FMM algorithm at all network loads. The performances of OLFT+EF and OLFT+NPFR are relatively similar at the network loads of 2000 to 5000 Erlang.

For 900 Gbps traffic, as depicted in Figs. 24(a) and 24(b), the OLFT+FMM has the highest BP and BBP values among all algorithms. The performances of the OLFT+EF and OLFT+NPFR algorithms are relatively similar. The performance of OLFT+DemFRAG is slightly better than OLFT+Fc at the network load of 2000 to 5000 Erlang.

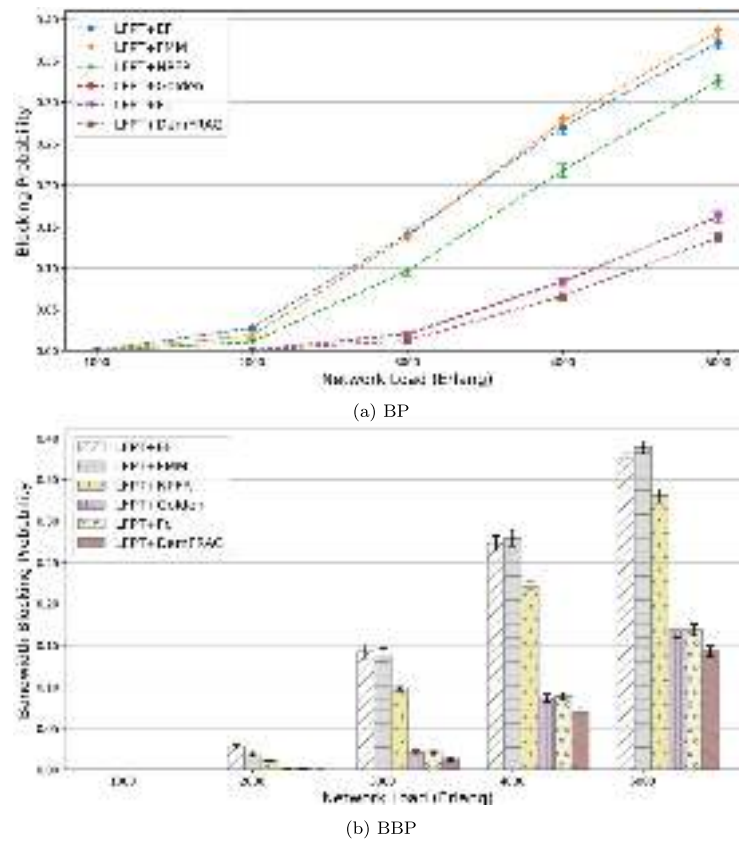


Fig. 15. Simulation results of LFPT-MRMSA under JPN12 topology at 300 Gbps traffic requests.

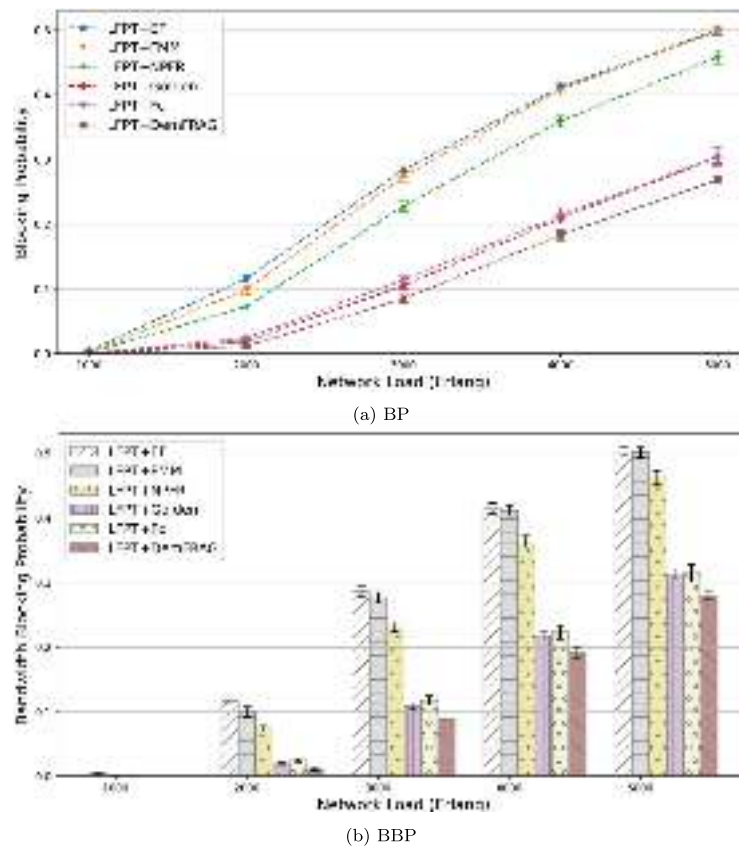


Fig. 16. Simulation results of LFPT-MRMSA under JPN12 topology at 400 Gbps traffic requests.

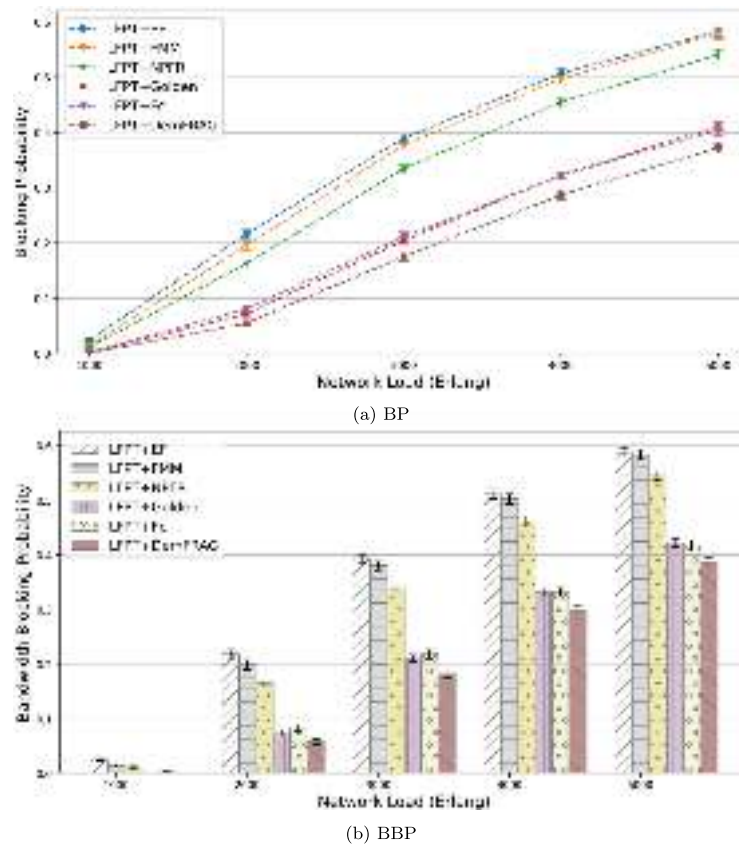


Fig. 17. Simulation results of LFPT-MRMSA under JPN12 topology at 500 Gbps traffic requests.

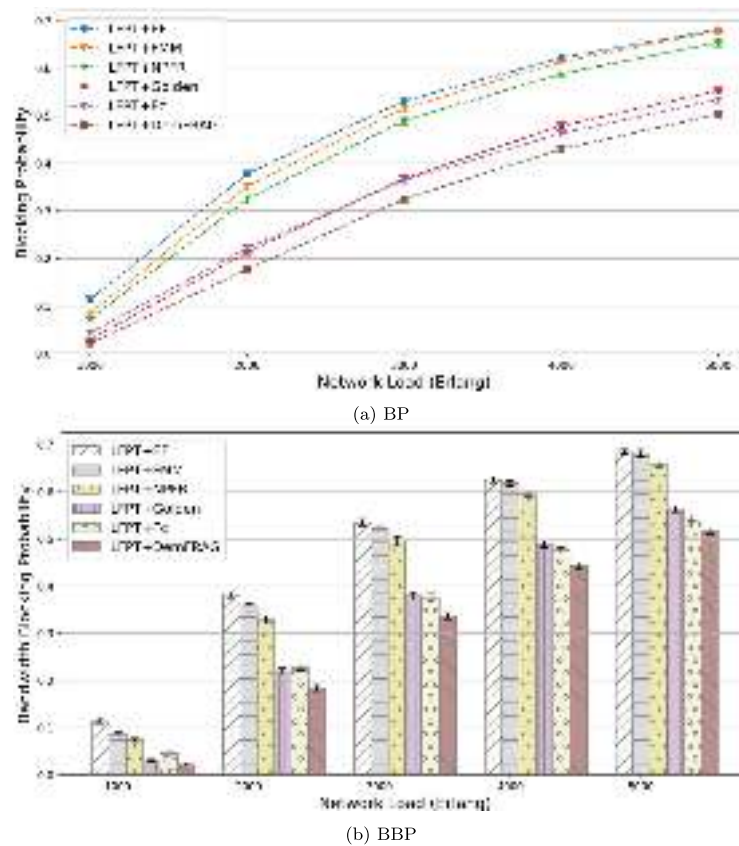


Fig. 18. Simulation results of LFPT-MRMSA under JPN12 topology at 700 Gbps traffic requests.

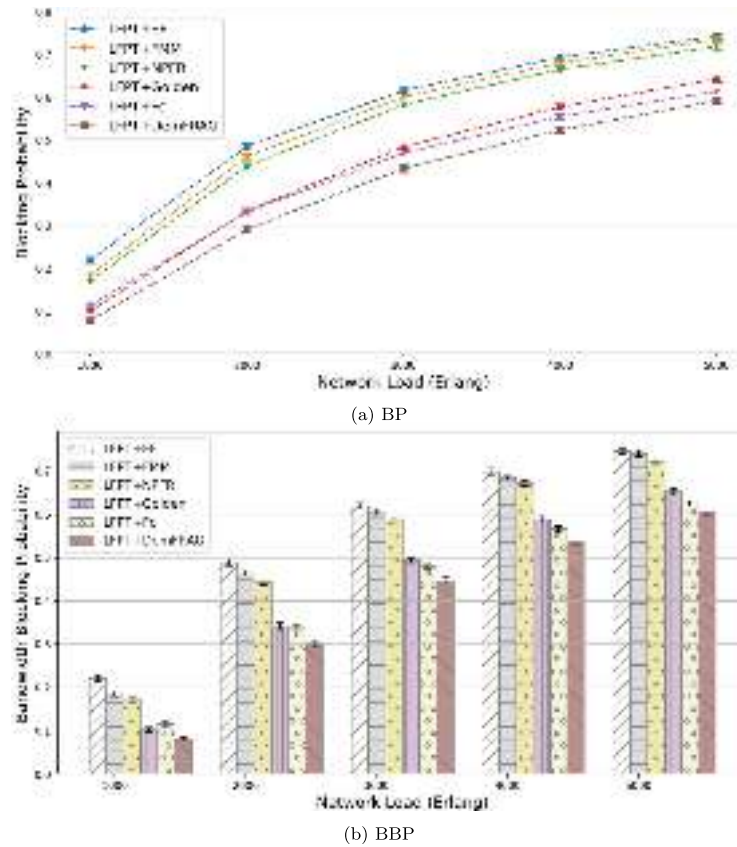


Fig. 19. Simulation results of LFPT-MRMSA under JPN12 topology at 900 Gbps traffic requests.

According to the results of simulation under JPN12, the OLFT-MRMSA algorithm with the DemFRAG and Fc metrics have relatively the same performance in reducing BP and BBP compared to other fragmentation metrics. This is due to the simple structure of JPN12 network compared to NSFNET. By considering bandwidth requirements of input requests, both the DemFRAG and Fc metrics can find the least fragmented multicast light-tree in the OLFT-MRMSA algorithm. We can obtain better results in the OLFT-MRMSA algorithm, by increasing total number of constructed multicast trees N_t .

5.3. Discussion on improvements of the DemFRAG metric

The results of simulation show that by using the DemFRAG metric in the LFPT-MRMSA and OLFT-MRMSA algorithms compared to other fragmentation metrics, under high data rates (300–900 Gbps), BP and BBP decrease significantly. As well as, The reductions in BP and BBP of the DemFRAG metric become more pronounced as data rate, network load, and network topology size increase. This is because of considering the size of demands and the impact of appropriate and inappropriate free frequency blocks in calculating the fragmentation degree of paths, and therefore, achieving more accurate value of fragmentation. Given this, the LFPT+DemFRAG and OLFT+DemFRAG algorithms have the best performance among the compared MRMSA algorithms with other fragmentation metrics.

We compute the average improvement of the DemFRAG metric in BP, relative to other fragmentation metrics, in the LFPT-MRMSA and OLFT-MRMSA algorithms at the network loads of 3000, 4000, and 5000 Erlang to better demonstrate its superiority in decreasing BP. Results are illustrated in Table 6. We discuss improvement of DemFRAG at 300 Gbps traffic type under the NSFNET and JPN12 topologies.

Under NSFNET, the LFPT+DemFRAG algorithm provides 90.8%, 90.2%, 89.2%, 78.6%, and 62.1% improvement in BP compared to the LFPT+EF, LFPT+FMM, LFPT+NPFR, LFPT+Golden, and LFPT+Fc

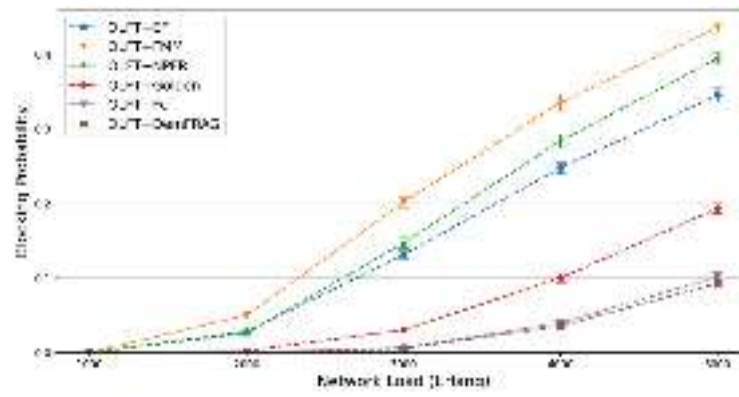
algorithms respectively. Under JPN12, the LFPT+DemFRAG algorithm provides 76.7%, 77.2%, 71.6%, 24.6%, and 26.0% improvement in BP compared to the LFPT+EF, LFPT+FMM, LFPT+NPFR, LFPT+Golden, and LFPT+Fc algorithms, respectively.

Under NSFNET, the OLFT+DemFRAG algorithm provides 81.3%, 82.9%, 81.4%, 63.2%, and 27.9% improvement in BP compared to the OLFT+EF, OLFT+FMM, OLFT+NPFR, OLFT+Golden, and OLFT+Fc algorithms respectively. Under JPN12, the OLFT+DemFRAG algorithm provides 84.8%, 88.4%, 86.7%, 66.0%, and 11.0% improvement in BP compared to the OLFT+EF, OLFT+FMM, OLFT+NPFR, OLFT+Golden, and OLFT+Fc algorithms, respectively.

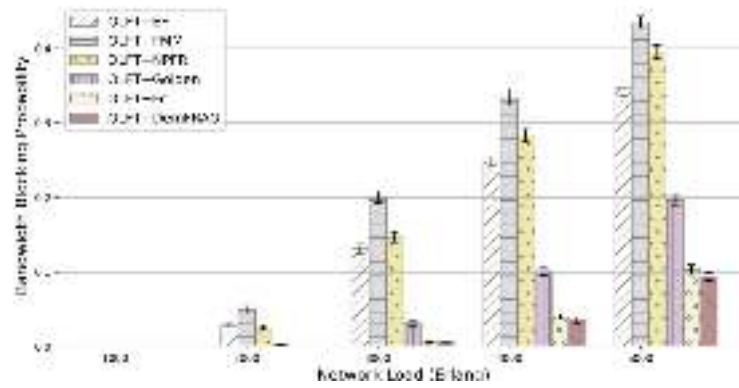
Achieved improvements are due to increasing spectral efficiency by using the DemFRAG metric, and therefore, reducing the BP value. Improvement of DemFRAG at 400, 500, 700, and 900 Gbps traffic types can be observed from presented results in Table 6. Similar computations can be carried out to illustrate improvements achieved by the DemFRAG metric in reducing BBP compared to other fragmentation metrics.

6. Conclusions

In this paper, we have proposed efficient fragmentation-aware algorithms for multicast routing, modulation level and spectrum assignment for dynamic multicast traffic with high data rates (300–900 Gbps) in EONs. We proposed a novel demand size based fragmentation metric (DemFRAG) that evaluates the fragmentation status of paths based on the required frequency slots of incoming multicast requests. We proposed two heuristic algorithms named Least Fragmented Path based Tree MRMSA (LFPT-MRMSA) algorithm and Optimal Least Fragmented Tree MRMSA (OLFT-MRMSA) algorithm that are fragmentation-aware methods based on our novel DemFRAG metric. The performance of the proposed fragmentation-aware LFPT-MRMSA and OLFT-MRMSA algorithms was compared with the other fragmentation-aware algorithms in

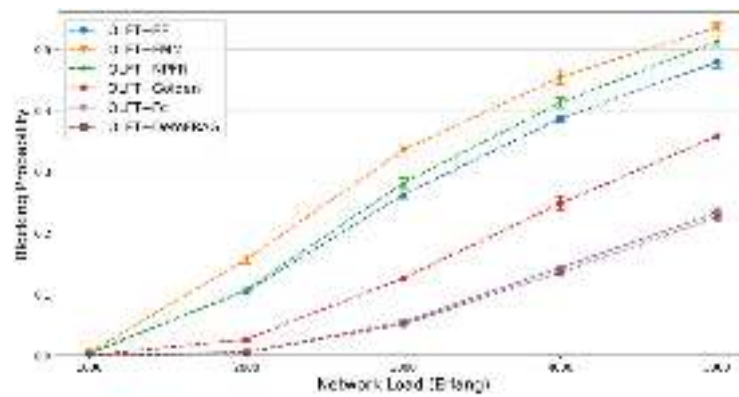


(a) BP

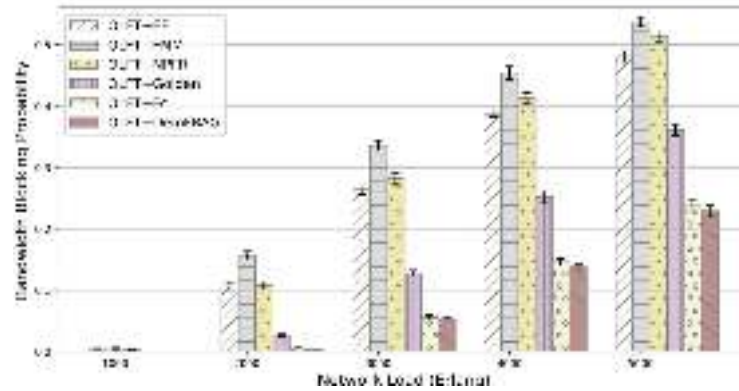


(b) BBP

Fig. 20. Simulation results of OLFT-MRMSA under JPN12 topology at 300 Gbps traffic requests.

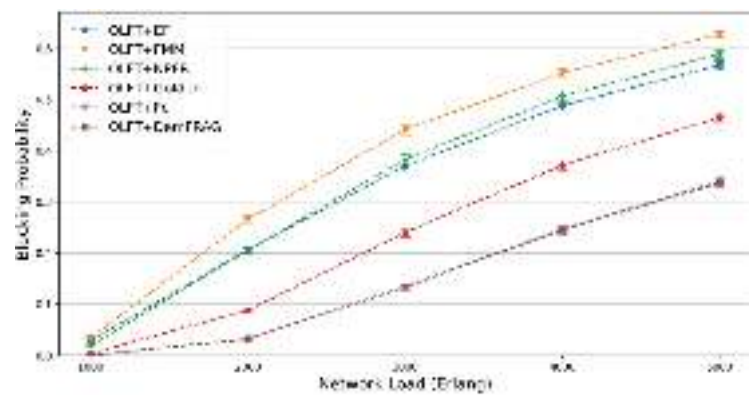


(a) BP

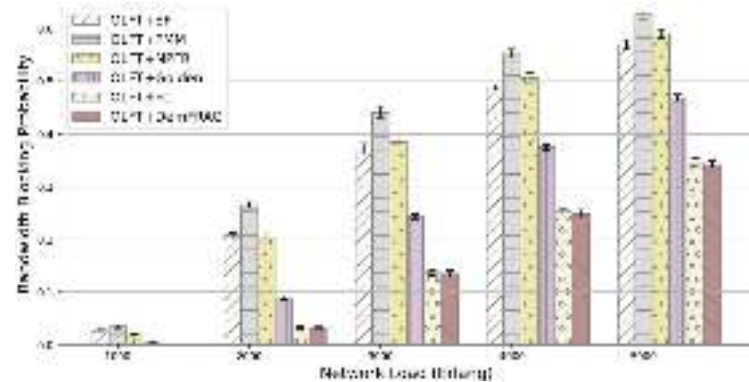


(b) BBP

Fig. 21. Simulation results of OLFT-MRMSA under JPN12 topology at 400 Gbps traffic requests.

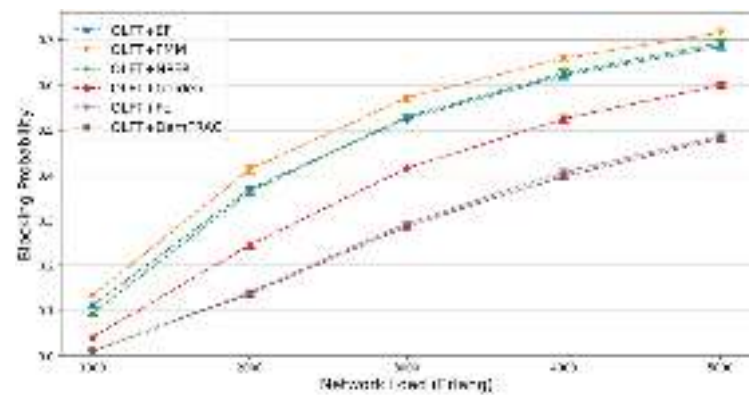


(a) BP

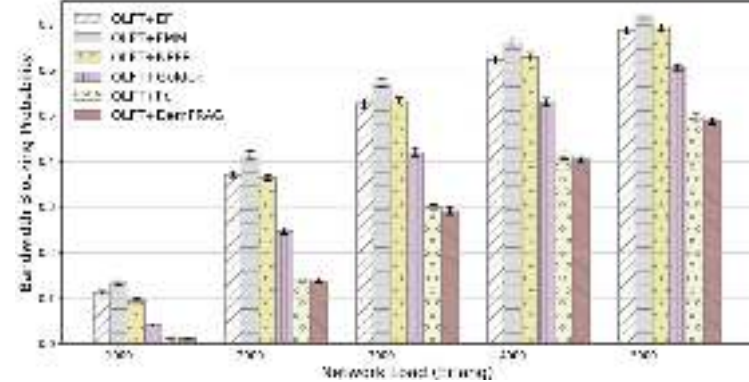


(b) BBP

Fig. 22. Simulation results of OLFT-MRMSA under JPN12 topology at 500 Gbps traffic requests.



(a) BP



(b) BBP

Fig. 23. Simulation results of OLFT-MRMSA under JPN12 topology at 700 Gbps traffic requests.

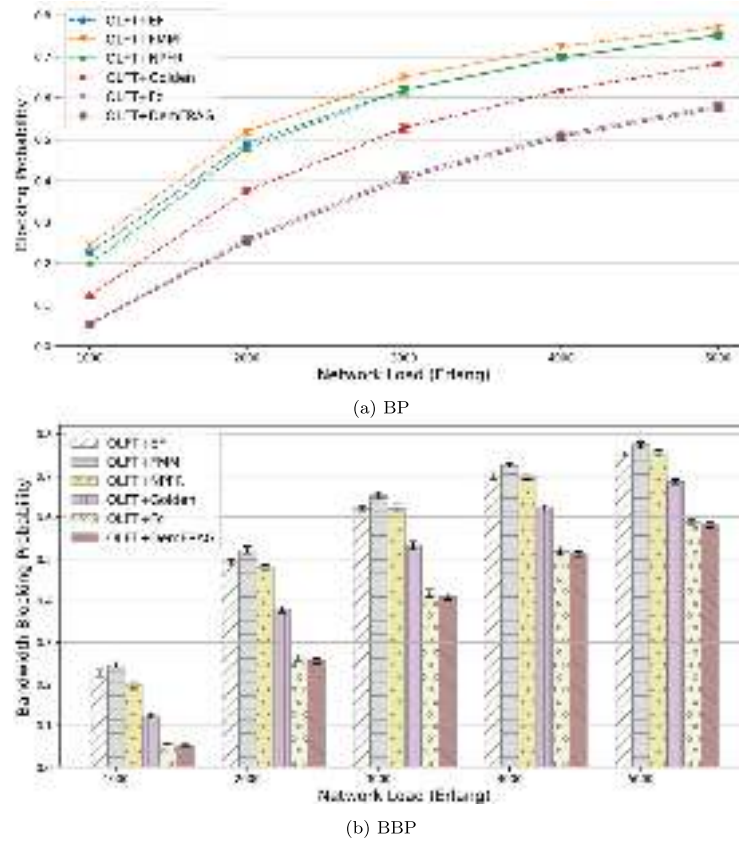


Fig. 24. Simulation results of OLFT-MRMSA under JPN12 topology at 900 Gbps traffic requests.

Table 6

The DemFRAG metric improvement in Blocking Probability (BP) compared to other fragmentation metrics.

Network	Algorithm	Traffic (Gbps)	EF	FMM	NPFR	Golden	Fc
NSFNET	LFPT-MRMSA	300	90.8%	90.2%	89.2%	78.6%	62.1%
		400	76.3%	74.3%	72.6%	56.6%	46.8%
		500	64.1%	61.4%	60.4%	42.9%	29.2%
		700	48.7%	44.5%	42.5%	30.2%	27.7%
		900	35.0%	31.7%	31.7%	19.1%	11.0%
JPN12	LFPT-MRMSA	300	76.7%	77.2%	71.6%	24.6%	26.0%
		400	57.4%	56.8%	51.1%	14.5%	17.3%
		500	44.8%	43.8%	38.5%	11.6%	11.9%
		700	31.9%	30.9%	27.9%	10.3%	7.9%
		900	24.8%	23.5%	21.5%	9.2%	5.6%
NSFNET	OLFT-MRMSA	300	81.3%	82.9%	81.4%	63.2%	27.9%
		400	65.3%	67.1%	64.5%	45.6%	16.0%
		500	54.6%	55.3%	53.2%	33.3%	11.0%
		700	40.9%	41.1%	37.8%	26.1%	6.6%
		900	31.9%	30.6%	28.9%	18.8%	2.4%
JPN12	OLFT-MRMSA	300	84.8%	88.4%	86.7%	66.0%	11.0%
		400	66.0%	70.8%	68.2%	47.1%	4.8%
		500	51.4%	57.2%	53.2%	35.4%	1.0%
		700	37.0%	40.7%	37.6%	25.0%	1.9%
		900	28.5%	31.1%	28.5%	19.0%	1.4%

terms of Blocking Probability (BP) and Bandwidth Blocking Probability (BBP) for different bandwidth requests and at various network loads under NSFNET and JPN12 topologies. The simulation results showed the superiority of the proposed algorithms with the DemFRAG metric over all other algorithms. By using the DemFRAG metric, compared to the other metrics, the BP and BBP values decrease. So we can conclude that our proposed novel DemFRAG fragmentation metric can evaluate the value of fragmented spectrum on lightpaths and light-trees very well.

CRedit authorship contribution statement

Leila Asadzadeh: Writing – original draft, Visualization, Methodology, Conceptualization. **Ahmad Khonsari:** Supervision, Developing main idea of the study. **Akbar Ghaffarpour Rahbar:** Writing – review & editing, Project administration, Supervision.

Declaration of competing interest

The authors declare that they have no known competing financial interests or personal relationships that could have appeared to influence the work reported in this paper.

Data availability

No data was used for the research described in the article.

References

- [1] W. Kmieć, R. Gościń, K. Walkowiak, M. Klinkowski, Two-layer optimization of survivable overlay multicasting in elastic optical networks, *Opt. Switch. Netw.* 14 (2014) 164–178.
- [2] M. Molnár, D.D. Le, J. Perelló, J. Solé-Pareta, C. McArdle, Multicast routing from a set of data centers in elastic optical networks, *Opt. Switch. Netw.* 34 (2019) 35–46.
- [3] M. Tarhani, S. Sarkar, M.K. Eghbal, M. Shadaram, Efficient multicasting technique for elastic optical network, *IET Netw.* 4 (2021) 250–257.
- [4] B.C. Chatterjee, N. Sarma, E. Oki, Routing and spectrum allocation in elastic optical networks: a tutorial, *IEEE Commun. Surv. Tutor.* 17 (3) (2015) 1776–1800.
- [5] M.Sh. Aboomasoudi, A. Avokh, Improving acceptance rate of QoS-guaranteed point-to-multipoint traffic flows in elastic optical networks, *Opt. Fiber Technol.* 59 (2020).
- [6] L. Ruiz, R.J. Durán Barroso, I. De Miguel, N. Merayo, J.C. Aguado, E.J. Abril, Routing, modulation and spectrum assignment algorithm using multi-path routing and best-fit, *IEEE Access* 9 (2021) 111633–111650.
- [7] J. Sócrates-Dantas, R.M. Silveira, D. Careglio, J.R. Amazonas, J. Solé-Pareta, W.V. Ruggiero, A study in current dynamic fragmentation-aware RSA algorithms, in: 2014 16th International Conference on Transparent Optical Networks, ICTON, Graz, Austria, 2014, pp. 1–4.
- [8] M. Jafari-Beyrami, A. Ghaffarpour Rahbar, S. Hosseini, On-demand fragmentation-aware spectrum allocation in space division multiplexed elastic optical networks with minimized crosstalk and multipath routing, *Comput. Netw.* 181 (2020).
- [9] Y. Khorasani, A. Ghaffarpour Rahbar, M. Jafari-Beyrami, A novel two-dimensional metric for fragmentation evaluation in elastic optical networks, *Comput. Netw.* 216 (2022).
- [10] F. Yousefi, A. Ghaffarpour Rahbar, M. Yaghubi-Namaad, Fragmentation-aware algorithms for multipath routing and spectrum assignment in elastic optical networks, *Opt. Fiber Technol.* 53 (2019).
- [11] K. Walkowiak, A. Kasprzak, M. Woźniak, Algorithms for calculation of candidate trees for efficient multicasting in elastic optical networks, in: 2015 17th International Conference on Transparent Optical Networks, ICTON, Budapest, Hungary, 2015, pp. 1–4.
- [12] M. Moharrami, H. Beyranvand, A. Fallahpour, J.A. Salehi, Spectrum-usage-aware resource allocation and multicast routing in elastic optical networks, in: 2016 8th International Symposium on Telecommunications, IST, Tehran, Iran, 2016, pp. 45–50.
- [13] P.D. Choudhury, R.S. Chauhan, P.V. Sudheer, T. De, Multicast routing and spectrum assignment in flexible-grid optical networks based on light-tree sharing approach, in: 2016 International Conference on Information Technology, ICIT, Bhubaneswar, India, 2016, pp. 173–179.
- [14] M. Guo, J. Yuan, Q. Zhang, X. Li, S. Nan, Link-aware distributed steiner sub-tree scheme for all-optical multicasting in elastic optical datacenter networks, *Opt. Fiber Technol.* 74 (2022).
- [15] X. Li, L. Zhang, Y. Tang, J. Guo, S. Huang, Distributed sub-tree-based optical multicasting scheme in elastic optical data center networks, *IEEE Access* 6 (2018) 6464–6477.
- [16] Z. Fan, Y. Li, G. Shen, C.-K.C. Chan, Distance-adaptive spectrum resource allocation using subtree scheme for all-optical multicasting in elastic optical networks, *J. Lightwave Technol.* 35 (9) (2017) 1460–1468.
- [17] A. Cai, K. Xu, M. Zukerman, Comparison of different multicast approaches in elastic optical networks, in: 2018 20th International Conference on Transparent Optical Networks, ICTON, Bucharest, Romania, 2018, pp. 1–4.
- [18] A. Cai, Y. Li, J. Chen, J. Shen, Coordinating multiple light-trails in multicast elastic optical networks with adaptive modulation, *IEEE Photonics J.* 15 (1) (2023) 1–15.
- [19] M. Firdhous, Multicasting over overlay networks-a critical review, *Int. J. Adv. Comput. Sci. Appl.* 2 (3) (2011) 54–61.
- [20] X. Liu, L. Gong, Z. Zhu, On the spectrum-efficient overlay multicast in elastic optical networks built with multicast-incapable switches, *IEEE Commun. Lett.* 17 (9) (2013) 1860–1863.
- [21] W. Kmieć, K. Walkowiak, Dynamic overlay multicasting for deadline-driven requests provisioning in elastic optical networks, in: 2017 20th Conference on Innovations in Clouds, Internet and Networks, ICIN, 2017, pp. 31–35.
- [22] X. Liu, L. Gong, Z. Zhu, Design integrated RSA for multicast in elastic optical networks with a layered approach, in: 2013 IEEE Global Communications Conference, GLOBECOM, Atlanta, GA, USA, 2013, pp. 2346–2351.
- [23] S. Sarraf-Maralaniyan, A. Ghaffarpour Rahbar, *MT³A*: a novel multicast routing, spectrum and modulation-level assignment in elastic optical networks, *Comput. Netw.* 218 (2022).
- [24] R. Gościń, M. Kucharszak, On the efficient optimization of unicast, anycast and multicast flows in survivable elastic optical networks, *Opt. Switch. Netw.* 31 (2019) 114–126.
- [25] K. Walkowiak, R. Gościń, M. Klinkowski, M. Woźniak, Optimization of multicast traffic in elastic optical networks with distance-adaptive transmission, *IEEE Commun. Lett.* 18 (12) (2014) 2117–2120.
- [26] Q. Wang, L.-K. Chen, Performance Analysis of Multicast Traffic Over Spectrum Elastic Optical Networks, OFC/NFOEC, Los Angeles, CA, USA, 2012, pp. 1–3.
- [27] P.D. Choudhury, P.V.R. Reddy, B.C. Chatterjee, E. Oki, T. De, Performance of routing and spectrum allocation approaches for multicast traffic in elastic optical networks, *Opt. Fiber Technol.* 58 (2020).
- [28] Y. Liu, X. Liu, J. Zhang, Y. Cao, X. Liu, Research on load balancing algorithm of multicast services based on EON, in: 2020 IEEE 6th International Conference on Computer and Communications, ICC, Chengdu, China, 2020, pp. 764–770.
- [29] Y. Qiu, Time based resource-consumption-aware spectrum assignment for multicast traffic in elastic optical networks, *Opt. Fiber Technol.* 59 (2020).
- [30] Y. Tang, X. Li, T. Gao, L. Zhang, S. Huang, Cost-adaptive multi-class multicast service aggregation based on distributed sub-trees in elastic optical data center networks, *Opt. Fiber Technol.* 66 (2021).
- [31] M. Aibin, K. Walkowiak, Different strategies for dynamic multicast traffic protection in elastic optical networks, in: 2016 8th International Workshop on Resilient Networks Design and Modeling, RNDM, 2016, pp. 174–180.
- [32] T. Gao, W. Zou, X. Li, B. Guo, Sh. Huang, B. Mukherjee, Distributed sub-light-tree based multicast provisioning with shared protection in elastic optical datacenter networks, *Opt. Switch. Netw.* 31 (2019) 39–51.
- [33] A. Cai, Z. Fan, K. Xu, M. Zukerman, C.-K. Chan, Elastic versus WDM networks with dedicated multicast protection, *J. Opt. Commun. Netw.* 9 (11) (2017) 921–933.
- [34] M. Pan, Y. Qiu, C. Zhang, Multiple leaf-ringing based protection algorithm with spectrum defragmentation for multicast traffic in elastic optical network, *Opt. Fiber Technol.* 61 (2021).
- [35] Mandloi A. Vasundhara, M. Patel, Fragmentation coefficient (FC) conscious routing, core and spectrum allocation in SDM-EON based on multicore fiber, in: 2023 2nd International Conference on Paradigm Shifts in Communications Embedded Systems, Machine Learning and Signal Processing, PCEMS, Nagpur, India, 2023, pp. 1–4.
- [36] Mandloi A. Vasundhara, Routing and dynamic core allocation with fragmentation optimization in EON-SDM, *Opt. Fiber Technol.* 83 (2024).
- [37] S. Zhang, X. Ren, Y. Zhao, Y. Guo, C. Yang, X. Xue, Spectrum fragmentation evaluation and dynamic bandwidth allocation for elastic optical networks, in: 2023 21st International Conference on Optical Communications and Networks, ICOON, Qufu, China, 2023, pp. 1–3.
- [38] M. Hafezi, A. Ghaffarpour Rahbar, Fragmentation-aware with core classification algorithms for spectrum allocation in elastic optical networks-space division multiplexing (SDM-EON), *Opt. Fiber Technol.* 82 (2024).
- [39] E. Oki, B.C. Chatterjee, Design and control in elastic optical networks: issues, challenges, and research directions, in: Proceedings of the International Conference on Computing, Networking and Communications, ICNC, IEEE, 2017, pp. 546–549.
- [40] A. Rosa, C. Cavdar, S. Carvalho, J. Costa, L. Wosinska, Spectrum allocation policy modeling for elastic optical networks, in: High Capacity Optical Networks and Emerging/Enabling Technologies, Istanbul, Turkey, 2012, pp. 242–246.
- [41] J. Zhao, B. Bao, B.C. Chatterjee, E. Oki, J. Hu, D. Ren, Dispersion based highest modulation- first last-fit spectrum allocation scheme for elastic optical networks, *IEEE Access* 6 (2018) 59907–59916.